IEEE Access
Multidisciplinary | Rapid Review | Open Access Journal

Received January 21, 2021, accepted February 7, 2021, date of publication February 11, 2021, date of current version February 23, 2021.

Digital Object Identifier 10.1109/ACCESS.2021.3058733

Non-Invasive Fetal Electrocardiogram Extraction Based on Novel Hybrid Method for Intrapartum ST Segment Analysis

RADEK MARTINEK[1], (Member, IEEE), RADANA KAHANKOVA[1], RENE JAROS[1], KATERINA BARNOVA[1], ADAM MATONIA[2], MICHAL JEZEWSKI[3], ROBERT CZABANSKI[3], KRZYSZTOF HOROBA[2], AND JANUSZ JEZEWSKI[2], (Senior Member, IEEE)

[1]Department of Cybernetics and Biomedical Engineering, Faculty of Electrical Engineering and Computer Science, VSB—Technical University of Ostrava, 708 33 Ostrava, Czech Republic
[2]Łukasiewicz Research Network—Institute of Medical Technology and Equipment, 41800 Zabrze, Poland
[3]Department of Cybernetics, Nanotechnology and Data Processing, Silesian University of Technology, 44100 Gliwice, Poland

Corresponding author: Rene Jaros (rene.jaros@vsb.cz)

This work was supported in part by the Ministry of Education of the Czech Republic under Project SP2021/32, and in part by the European Regional Development Fund in the Research Centre of Advanced Mechatronic Systems project through the Operational Programme Research, Development and Education under Project CZ.02.1.01/0.0/0.0/16_019/0000867.

ABSTRACT This study focuses on non-invasive fetal electrocardiogram extraction based on a novel hybrid method, which combines the advantages of non-adaptive and adaptive approaches for non-invasive fetal electrocardiogram morphological analysis. Besides estimating fetal heart rate, which is the main parameter used in the clinical practice, this study provides non-invasive ST segment analysis on data from Abdominal and Direct Fetal Electrocardiogram Database consisting of simultaneous traditional - gold standard invasive fetal scalp electrode and non-invasive fetal electrocardiogram recorded during delivery. This innovative approach utilizing the combination of independent component analysis and recursive least squares algorithms has the potential to extract valuable information from non-invasive fetal electrocardiogram in order to identify eventual sign of fetal distress. This was a prospective observational study of non-invasive fetal electrocardiogram, using 4 abdominally sited electrodes, against the traditional fetal scalp electrode on 8 patients. In terms of fetal heart rate estimation, the accuracy was high for all 8 tested patients with average value equaled 0.20 beats per minute and average value of 1.96 standard deviation equaled 5.80 beats per minute. In 7 patients, it was possible to perform the ST segment analysis with high accuracy in determining T/QRS in comparison with the reference fetal scalp electrode signal with average values and 1.96 standard deviation equaled 0.008 and 0.031 respectively. This study thus demonstrates that ST segment analysis is feasible using non-invasive fECG using the proposed hybrid method.

INDEX TERMS Non-invasive fetal electrocardiography (NI-fECG), fetal heart rate (fHR), ST segment analysis (ST-analysis), hybrid method (HM), independent component analysis and recursive least squares (ICA-RLS), electronic fetal monitoring (EFM), fetal distress (FD), fetal scalp electrode (FSE).

I. INTRODUCTION

Electronic fetal monitoring (EFM) is an essential part of modern obstetrics, serving mainly to diagnose fetal distress (FD). Conventional EFM methods, such as cardiotocography (CTG), have been used over the last decades in clinical practice mainly for continuous fetal heart rate (fHR) monitoring during labor but also for the intermittent assessment during pregnancy [1], [2]. However, several studies [3]–[5] show that CTG is not sufficiently accurate and conclusive and is burdened with a large inter- and extra-observer disagreement [6], [7]. This is demonstrably one of the reasons for inappropriate diagnosis of fetal distress and consequently, high number of unnecessarily performed caesarean sections.

The associate editor coordinating the review of this manuscript and approving it for publication was Filbert Juwono.

For these reasons, physicians are demanding conceptually new solutions for non-invasive diagnostic methods [8].

Fetal electrocardiography (fECG) is among the most promising EFM methods. The main reason is that the fECG signal carries valuable information as changes in the morphology of the fECG waveform which are associated with dysfunction induced by FD [9]–[11]. Therefore, ST segment analysis of the fECG has been developed to provide objective information about the fetal condition as an adjunct to fHR monitoring [1], [12]. Two large randomized clinical trials showed a significantly lower rate of metabolic acidosis at birth and fewer operative deliveries for FD when CTG and ST analysis were used simultaneously [13], [14]. Metabolic dysfunction induced by FD might be reflected in fECG waveform as ST segment changes, such as an increase in T wave, which can be quantified by the ratio of the T wave to the QRS amplitude (T/QRS ratio) [15]. Simultaneous monitoring of fHR and ST segment analysis can thus help to reduce uncertainty of FD diagnosis and thus a number of unnecessarily performed caesareans for patients with suspected FD [1].

In non-invasive fetal electrocardiography (NI-fECG) based monitoring, fetal health state is assessed using the information extracted from the electrical potentials produced by the fetal heart, which are recorded by means of electrodes placed on the maternal abdomen. However, in these recordings, fetal electrocardiogram (fECG) is accompanied by maternal electrocardiogram (mECG) and a significant amount of noise [16]. Unfortunately, the magnitude of the fetal component is low compared to maternal one. Moreover, the signals overlap in time as well as frequency domain making the accurate extraction or morphological analysis of the fECG waveform a challenging task [16]–[18]. The resulting quality of fECG extraction has a major impact on both the accuracy of fHR estimation and extraction of the PQRST waves. In this study, a novel method of ST segment analysis is presented, which makes also possible further morphological analysis of other fECG features, such as QT interval [19]. Abnormalities in the fetal QT interval indicate electrophysiological changes in the myocardium. Long QT syndrome is a condition in which repolarization of the heart is affected. It results in an increased risk of an arrhythmia which can result in sudden infant death syndrome and fetal hypoxia [19]–[22].

A number of NI-fECG extraction methods have been introduced in the past, including principal component analysis (PCA) [23], [24], independent component analysis (ICA) [23], [25], wavelet transform (WT) [26], adaptive neuro-fuzzy inference system (ANFIS) [27] or least mean squares (LMS) and recursive least squares (RLS) algorithms [28]. Recent studies [29]–[32] have shown that hybrid methods (HM), which combine the advantages of non-adaptive and adaptive approach to fECG extraction, achieve greater accuracy in fECG extraction than when using the methods individually. However, most algorithms presented in these studies as well as the previous research of the authors' team presented in [23], [28]–[30], were able to obtain only a small portion of the large information potential of NI-fECG; their main aim was to determine fetal R positions and use them to estimate the fHR.

Recent studies [12], [33], [34] show the possibility to extract additional clinically relevant information from NI-fECG. However, to obtain a fECG signal of a sufficient quality to perform morphological analysis, it is necessary to select extraction methods more carefully so that the process does not deform the signal's morphology. In our previous works [29], [30], we achieved the best results using the ICA-RLS-WT algorithm, combining three different algorithms (ICA, RLS, and WT). However, in the last step the WT was applied to highlight the R peaks for more accurate fHR estimation which caused distortion of the fECG signal morphology and thus loss of important diagnostic information. For this reason, the study introduced herein performs the ST analysis on NI-fECG signals extracted with a help of ICA-RLS algorithm comprising the ICA and RLS methods.

In addition to the selection of suitable extraction method, it is necessary to pay attention to algorithm settings. Authors of [35] focus on optimization approaches for different filtering methods, however, their research relates mainly to the R-R interval detection. Such setting is thus applicable for further morphological analysis and will be a subject of our research.

Finally, it is necessary to choose the appropriate database to test the method's efficacy. Unfortunately, lack of publicly available databases with high quality abdominal recordings makes the NI-fECG research difficult. Current databases provide recordings that are either of insufficient length or quality [36]. Moreover, each of the database differs in the electrode placement and acquisition system configuration, as the location and number of electrodes is not standardized as is the case with classical ECG [36]. The effect of electrode placement and data acquisition quality on the efficacy of fECG extraction have been demonstrated in [28], [37]. Thus, to ensure accurate morphological analysis, the recordings should not contain a significant amount of noise, the fetal/maternal component ratio should be high enough, and the polarity of the signals should be unified.

Some authors [38] introduced synthetic signal generators to produce data for their experiments, however, the results obtained using artificial test signals often differ from those performed on real signals. In this study, the *Abdominal and Direct Fetal ECG Database* (ADFECGDB) [39], [40] was selected to test the proposed HM. This database is suitable for the objectives established since it includes both abdominal and reference scalp signals, recorded invasively during the labor by means of fetal scalp electrode. The reference signal can be considered as a gold standard because it allows us to obtain reference PQRST waves, determine T/QRS ratio and thus evaluate the accuracy of the NI- ST-analysis.

II. STATE OF THE ART

Morphological analysis of the fECG signal, acquired by internal monitoring, can be performed by means of STAN® (Neoventa Medical AB, Mölndal, Sweden). STAN

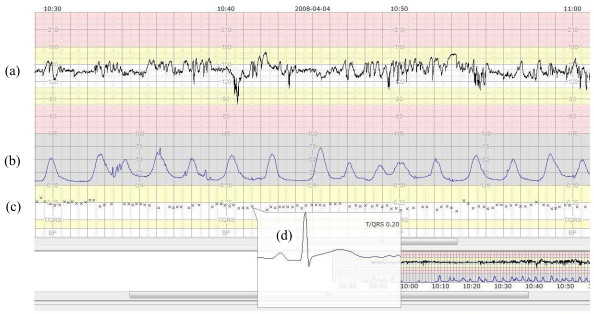

FIGURE 1. Example of the STAN monitor output: (a) fHR trace, (b) uterine contractions (toco), (c) T/QRS trace, and (d) example of the averaged T/QRS.

is an analysis tool for fetal monitoring, which combines ST-Analysis and CTG, providing extended and more accurate information about the fetus during labor than the CTG alone. An example of the STAN monitor output is shown in Fig. 1. The fECG is an invasive procedure in which the fHR is continuously calculated using the detected fQRS complexes, and ST segment analysis is performed by monitoring changes in the T/QRS ratio [36]. Nevertheless, the fECG can be performed only during the labor (after rupture of membranes) since it requires the FSE to be attached on the fetal head or hip decreasing comfort of the patient. The invasive fetal monitoring is also warranted in several risks that include infection or bruising of the fetus [41]. For these reasons, the benefits of this method are often questioned [42], [43].

A. MORPHOLOGICAL ANALYSIS

Although the NI-fECG research has been significantly evolving in the past decade and novel extraction algorithms are constantly emerging, the efficiency of the filtration process remains assessed solely on the basis of fHR estimates [36]. Most of the contributions claim to obtain excellent results in fHR determination, however, this evaluation does not reflect the extraction efficiency in terms of signal morphology. Nevertheless, several attempts were made to extract the morphological features from the NI-FECG [44]. Their results can be summarized as follows:

- In [1], the authors reviewed the development of a three-stage methodology. In the first stage, the fHR was extracted from the abdominal ECG signals (aECGs) using a nonlinear analysis. In the second stage, a blind source separation technique was applied to obtain the fECG. Finally, monitoring of the fetus was implemented using features extracted from both the fHR and fECG morphology (the T/QRS ratio and the fetal ST waveforms characteristics). Synthetic recordings were used for the experiments.
- The authors of [45] used an algorithm based on the optimal-shrinkage under the wave-shape manifold model to extract fECG. Both fHR and signal morphology (PR, QT and ST intervals) were analyzed during the experiments on a dataset including real and simulated signals indicating the physiological and pathological condition of fetuses (e.g. fetal arrhythmia).
- In study presented in [46], the authors dealt with the detection of fetal arrhythmias. The type of arrhythmia was determined based on the estimated P-wave morphology. Blocked normal P wave can be associated with the presence of second-degree AV block. The analysis was performed on 500 real recordings.
- The authors of the study introduced in [44] tested three classes of NI-FECG extraction algorithms: blind source separation, template subtraction and adaptive methods. In addition to the detection of fQRS complexes, the problem of determination of QT interval length and T/QRS ratio was considered. The experiments were performed only on synthetic data.
- In a study presented in [47], the authors introduced Bayesian filtering framework based on the extended Kalman filter. Synthetic data was used for the evaluation based on determining the length of the QT interval.
- In [48] the fECG signal was extracted using the Kalman filter framework. The fHR estimation and ST segment analysis were performed based on real recordings.
- In [20] the authors performed QT interval analysis on real recordings using model-based estimation method. First, R peaks were detected based on threshold value and RR intervals were determined. Subsequently, the interval, in which the T wave should occur, was calculated. The end of the T wave was calculated as the median of this interval. The beginnings of the Q peaks were determined manually. The difference between QT intervals obtained by means of reference methods (scalp fECG and Doppler Ultrasound) was less than 5%. The effect of QT prolongation in bradycardia and long QT syndrome has been demonstrated.
- In [19], the authors performed QT interval analysis using a STAN S21 device on 68 fetuses that showed signs of metabolic acidosis at birth (pH $<$ 7.05). Approximately the same number of patients was used as a control group. The measurements were taken at the beginning of the recording (on the fHR baseline), during decelerations and at the end of the recording. The QT parameter was calculated by Bazett's formula and the determined intervals were compared using Wilcoxon test. The results confirmed that there is a significant shortening of the QT interval during severe intrapartum hypoxia and metabolic acidosis and thus proved that intrapartum QT interval monitoring may provide additional information on the condition of the fetus.
- Fetal QT interval analysis on non-invasive abdominal recordings was also part of the Challenge 2013 call [49]. For this purpose, a dataset was created containing recordings from different sources, with variable gestational age and electrode placement. The accuracy of the fetal QT interval estimation was evaluated using the root mean square difference between the reference and the calculated QT intervals. In the reference recordings,

fetal QT intervals were determined by an expert [49]. The best results were achieved by authors of [50].

The results of all these studies indicate that morphological analysis using NI-fECG is possible and provides results as obtained by invasive variant of fECG. However, quality aECG recordings must be used, filtering methods and settings that do not cause signal distortion must be appropriately selected, and suitable methods must be chosen for the correct detection of individual waves and oscillations in the fECG signal.

B. METHODS FOR fECG SIGNAL EXTRACTION

The challenge in processing and analyzing fECG is to extract the high quality fetal component from aECG signals. In the past, many authors [51]–[56] designed and tested methods that could suppress the interference contained in the aECG signal (especially the mECG component) and highlight the fECG component as much as possible.

- *Wavelet transform* is one of the most commonly used methods for fECG extraction, mainly due to the possibility of signal analysis in the time-frequency domain. To obtain optimal results, it is necessary to pay attention to the system setting, namely to the selection of the mother wavelet, its scale, and the number of decomposition levels. For the purposes of fECG extraction, the method was tested in [51], [57], where *Daubechies* wavelet was selected; in [58], the *Symlet* wavelet was found as suitable for fECG extraction; in [59] the authors concluded the *Biorthogonal* wavelet as the most effective wavelet base type for the fECG extraction.
- *Empirical mode decomposition based methods* - the principle of EMD based methods is based on the decomposition of the input signal into simpler signals, which are called intrinsic mode functions (IMFs). By selecting one or more IMFs and summing them, it is possible to create the filtered fECG signal. The basic EMD method achieved a relatively high-quality extraction of fECG in the [60], [61]. The extraction was further improved by using improved variants of this method, such as ensemble empirical mode decomposition (EEMD) [60], [61], complementary ensemble empirical mode decomposition (CEEMD) [60], [61], or complementary ensemble empirical mode decomposition with adaptive noise (CEEMDAN) [62].
- *Kalman filtering* - this method estimates the useful signal from noisy data based on the most recently measured data, the system model, but also using data on the previous state of the system. The disadvantage of the basic version of the filter is that it can be used only for linear systems. For practical use, an extended Kalman filter (EKF) and extended Kalman smoother (EKS) have been developed, which can also be used for nonlinear systems. Both filter variants, EKF and EKS, demonstrated their effectiveness in mECG component suppression and fECG signal extraction in [53], [63], [64] and [54], respectively.
- *Artificial neural networks* are used for parallel data processing based on mimicking the behavior of biological structures. The use of convolutional neural networks (CNN) to remove noise from the fECG signal has been tested in [65] with very good results. High-quality fECG filtration was also achieved in [66], where dynamic neural networks (DNN) with FIR synapses were tested and analyzed. The adaptive neuro-fuzzy inference system (ANFIS), combining neural networks and fuzzy logic principles, was tested in [67]. The echo state networks (ESN) method was used for fECG filtering in [68] and achieved very high quality results.
- *Blind source separation methods* - these methods have received a great deal of attention in the past, as they have been successful in fECG extraction. The principle is based on the decomposition of the signal mixture (aECG) into the original source components (fECG, mECG, noise). These methods assume that the sources are statistically independent. The basic representatives include the ICA [23], [55], [69]–[72], PCA [23], [73] or the singular value decomposition (SVD) [74], [75]. From this group of methods, the ICA [23] method proved to be the most suitable for fECG extraction. Several extended variants of ICA have been introduced, such as joint approximate diagonalization of eigen-matrices (JADE) [76], [77], the very efficient FastICA algorithm [78]–[80] or the multidimensional ICA (MICA) method [81]. A comparison of the performance of several ICA based methods was performed in [82]. The authors analyzed the FastICA algorithm, JADE, the efficient version of the FastICA (EFICA) and the second order blind identification (SOBI), where EFICA proved to be most efficient for fECG extraction. Similarly, in [83], the authors compared different ICA based algorithms: FastICA based on kurtosis, FastICA based on negentropy and JADE method. The most accurate extraction of fECG was obtained using the JADE method, but the FastICA method was able to extract fECG faster. The resulting performance of ICA based algorithms is affected by the number of input signals. At the same time, the higher the number of input signals, the more accurately it is possible to obtain source signals. Most of the presented ICA based methods are multichannel, but there is also a single-channel variant presented in [45], [84], achieving very promising results in the extraction of fECG. Nevertheless, a larger number of input signals is associated with greater computational complexity and lower comfort for the pregnant subject when recorded.
- *Adaptive filters* - these filters are based on minimizing the error signal by automatically adjusting the filter coefficients. The error signal is defined as the difference between the desired output and the actual output of the algorithm. For fECG extraction, the mECG component (mECG), which can be recorded from the mother's chest or extracted from a mixture of aECG signals using

a blind source separation method (e.g. ICA), is modified to form the mECG component contained in the aECG signal. This modified mECG component is then subtracted from the aECG signal and fECG is obtained. The adaptive LMS algorithm uses mean square error minimization between the desired and actual output. The LMS filter in combination with WT was used to extract the fECG efficiently in [59], [85]. The combination of LMS and ICA also achieved promising results in [70]. Other extended variants of this filter normalized LMS (NLMS), delayed LMS (DLMS) and block LMS (BLMS) were compared in [86], where the best results were achieved using the BLMS algorithm. The adaptive RLS method, which uses the minimization of the total squared error between the desired and actual output, was tested in [87] for fECG filtering. The performance of the method was compared with LMS but better results were achieved with RLS algorithm. In [88], the performance of the method in fECG extraction was compared with NLMS, and even in this case better results were obtained with RLS. A total of nine combinations of cascading RLS, LMS and NLMS filters were tested in [56]. The most promising results were achieved by the combination of LMS and RLS methods.

A comparison different extraction methods for fHR determination, morphology bias and computational complexity is summarized in Table 1. The evaluation of individual parameters was performed as follows:

- *Accuracy of fHR determination* - this parameter was evaluated using high, medium and low categories, defined as:
  - *High* - the method was able to suppress all noise efficiently and in the statistical evaluation of fHR determination achieved the accuracy of $\geq$ 95% (based on the ACC, SE, PPV and F1 parameters).
  - *Medium* - the method was able to suppress most interference, but some residues decreased the values of ACC, SE, PPV and F1 reaching the accuracy of $\geq$ 80% in the statistical evaluation of fHR determination.
  - *Low* - the method was not able to sufficiently remove the interference and in the statistical evaluation of fHR achieved the accuracy of $<$ 80% was achieved using the parameters ACC, SE, PPV and F1.
- *Distortion of morphology* - determines morphology of the signal is distorted by the given method. If so, it is no longer possible to perform morphological analysis of the signal, if not, morphological analysis of the signal is possible.
- *Computational complexity* - the parameter was evaluated using the categories high, medium and low defined as follows:
  - *High* - the method is computationally intensive and cannot be used in real-time applications.
  - *Medium* - the method is computationally slightly more demanding and can be used in real-time applications after optimization.
  - *Low* - the method is not computationally demanding and can thus be used in real-time applications.

TABLE 1. Comparison of methods for fECG extraction.

Algorithm	Accuracy of fHR determination	Distortion of morphology	Computational complexity
WT	Medium	Yes	Low
EMD	Medium	Yes	Medium
CEEMD	High	Yes	High
ANFIS	High	Yes	High
ICA	Medium	No	Medium
PCA	Medium	No	Low
SVD	Low	No	Low
LMS	Medium	No	Low
RLS	High	No	Medium

C. FETAL HEART RATE TRACE AND ST ANALYSIS INTERPRETATION

Correct feature extraction is important for the subsequent fetal health assessment. This subsection will outline the clinical methodology for evaluating fHR traces and direct fECG recordings. These recommendations are used by the clinicians as well as in the fetal monitoring systems and devices based on fECG (e.g. STAN S31 and STAN S41).

In 2015, the FIGO published a new consensus guideline on intrapartum fetal monitoring (FIGO2015) [89] that modified the earlier version published in 1987 (FIGO1987) [90]. These new recommendations constituted the first wide-scale agreement on essential aspects of CTG monitoring. The purpose of the FIGO guidelines is to assist in the use and interpretation of CTG tracings [2], as well as in the clinical management of specific CTG patterns, such as baseline fHR, variability or decelerations [6], [7] (see Table 2). Moreover, the Swedish Society of Obstetrics and Gynecology (SSOG), issued their latest recommendations related to the same matter in 2017 [91] (SSOG2017).

The assessment is usually performed by obstetricians or midwifes who classify the tracings into one of three classes: normal, suspicious or pathological according to the criteria summarized in Table 2 [89]. The tracings should be reevaluated within a reasonable time frame (at least every 30 minutes) due to changing nature of CTG signals during labor [89], [92].

In addition to the above-mentioned evaluation parameters, further morphological analysis of the fECG waveform, especially ST-segment analysis (ST-analysis), has been proposed. Its objective was to improve the clinical use of EFM since various studies [13], [93]–[95] have demonstrated that it can provide information on oxygenation of the fetal myocardium [12]. Studies also linked adrenaline surge and the appearance of high T waves in the fetal ECG [96].

TABLE 2. CTG classification criteria, interpretation and recommended management according to FIGO consensus guidelines on intrapartum fetal monitoring.

	Normal	Suspicious	Pathological
Baseline	110–160 bpm		$<$ 100 bpm
Variability	5–25 bpm	Lacking at least one characteristic of normality.	Reduced variability. Increased variability. Sinusoidal pattern.
Decelerations	No repetitive[1] decelerations.	but with no pathological features.	Repetitive late or prolonged decelerations for $>$ 30 min (or $>$ 20 min if reduced variability). Deceleration $>$ 5 min.
Interpretation	No hypoxia/acidosis.	Low probability of hypoxia/acidosis.	High probability of hypoxia/acidosis.
Clinical management	No intervention necessary to improve fetal oxygenation state.	Action to correct reversible causes if identified, close monitoring or adjunctive methods.	Immediate action to correct reversible causes, adjunctive methods, or if this is not possible expedite delivery. In acute situations immediate delivery should be accomplished.

TABLE 3. Suggested Course of Action based on ST Events noted and Classification of CTG based on STAN Guidelines.

ST event	Intermediary CTG	Abnormal CTG	Preterminal CTG
Episodic T/QRS rise	$>$ 0.15	$>$ 0.10	
Baseline T/QRS rise	$>$ 0.10	$>$ 0.05	Immediate delivery
Biphasic ST	Three biphasic ST events	Two biphasic ST events	

Prolongation of the QRS interval was found to be associated with baseline tachycardia, shortening of the P-R interval with CTG decelerations, and T wave inversion with signs of placental dysfunction [97]. Additionally, Pardi *et al.* in [98] showed changes in ECG configuration during periods of fetal hypoxia, with P wave and P-Q interval modifications appearing consistently during late decelerations; ST depression/elevation/inversion or increased T wave amplitude occurred in 48% of cases.

Based on those findings and the recommendations for ST analysis evaluation published in [12], which were later taken over by Neoventa Medical to create their evaluation guide used in STAN analyzer, new categories of ST related events were identified including:

- Three categories of biphasic ST segments according to the relationship between the baseline and their slope:
  - 1 (slope above baseline),
  - 2 (crossing the baseline),
  - 3 (below baseline).
- Three types of relevant ST events, associated with acidosis and incorporated into signal processing algorithms:
  - episodic T/QRS rise (T/QRS rise $>$ 0.10 in 2 consecutive T/QRSs),
  - baseline T/QRS rise (T/QRS rise $>$ 0.05 in more than 10 minutes),
  - ST interval depressions: categories 2 and 3 biphasic ST events.

Currently, the clinical use of ST analysis requires it to be combined with CTG analysis [95], see Table 3. Homogeneity and agreement statistics between the CTG classifications SSOG2017, FIGO2015, and FIGO1987 were performed and published in [91]. The study aimed to reveal homogeneity and agreement between the systems in classifying CTG and ST events, and relate them to maternal and perinatal outcomes. The results showed discrepancies in the classification between the old and new systems.

III. MATERIAL AND METHODS

The aim of this study is to test and statistically evaluate the effectiveness of the hybrid ICA-RLS extraction method of fECG. The ICA method allows for separating the statistically independent signals and it has been already successfully used for the fECG extraction [25]. This algorithm is relatively computationally demanding; therefore, several faster variants of this method have been introduced [29], [99]. The most commonly used variant, the so-called FastICA algorithm, was successfully applied to extract the fECG from aECGs [72]. The RLS method is also an effective tool for the fECG extraction, as confirmed by [28], [100], but its main disadvantage is the high computational complexity. The background theory of ICA and RLS methods is well described in the literature [23], [28], [29], [78], [101], [102], and their detailed presentation will therefore not be included in this study.

[1]Decelerations are repetitive when associated with $>$ 50% contractions. Absence of accelerations in labour is of uncertain significance.

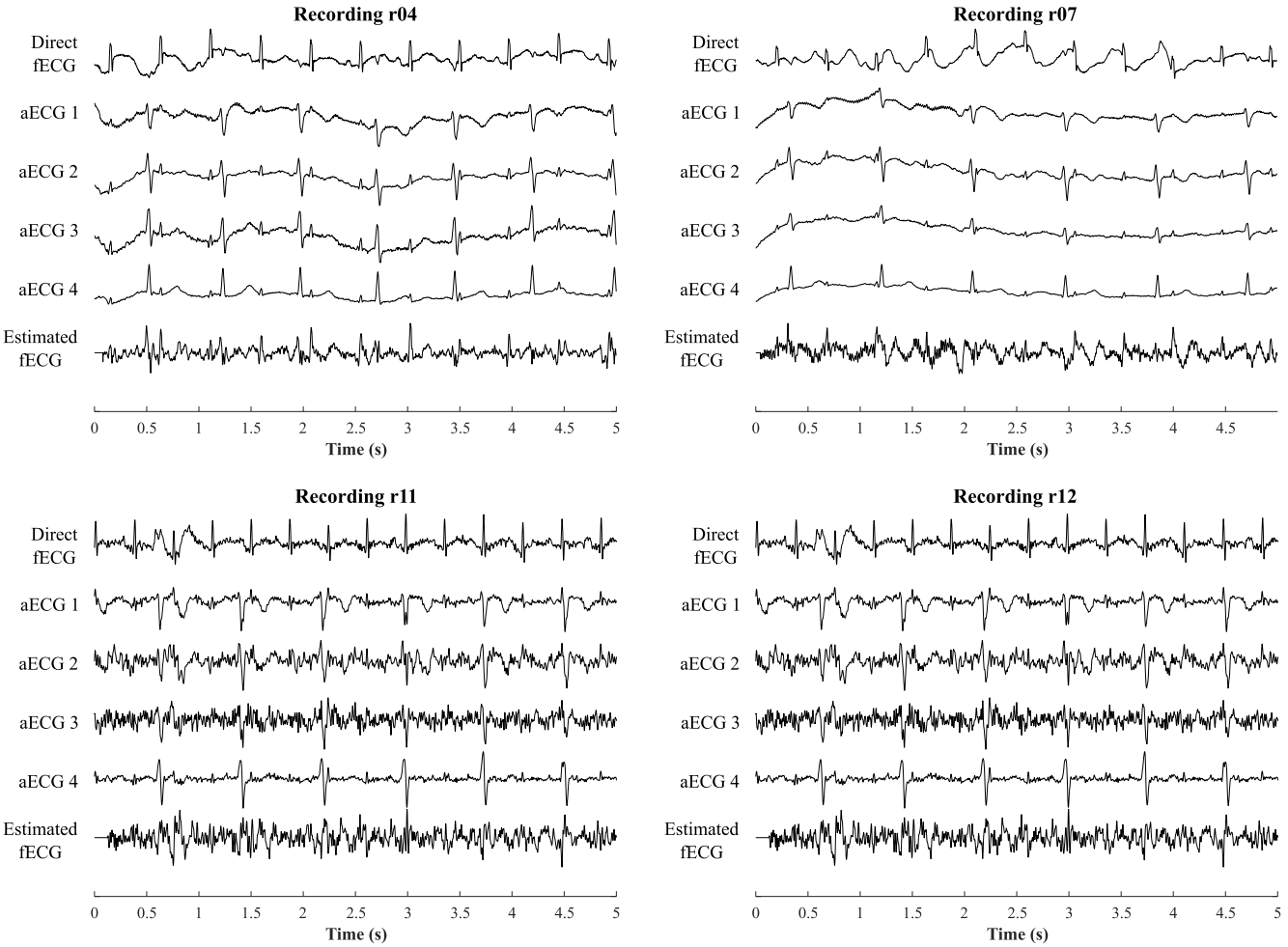

FIGURE 2. Examples of the omitted abdominal ECG signals (recordings r04, r07, r11, and r12) and estimated fECG signals.

This section will introduce only the hybrid ICA-RLS based system, the testing dataset, and the evaluation parameters and process.

A. DATASET

The hybrid method was tested using real data, as the assessment of extraction efficiency on synthetic signals is often misleading. In addition, it was necessary to select a database that includes a continuous reference scalp recordings in addition to abdominal ones so that the accuracy of the NI-fECG can be evaluated. Only one publicly available database (ADFECGDB) meets these criteria, thus we used it in our experiments [23], [39], [103]. These recordings were obtained from 12 subjects between the 38th and 41st week of pregnancy. Each includes four abdominal and one direct signal along with the annotations indicating the location of the fetal R peaks. These annotations were created by on-line analysis in the KOMPOREL system and verified by a group of cardiologists [39], [103]. The sampling frequency was 1000 Hz (for five recordings) and 500 Hz (for seven recordings), the signal resolution was 16 bits. The abdominal signals were recorded using the Ag-AgCl electrodes, while the direct signals were recorded by means of spiral fetal scalp electrode. The configuration of the abdominal electrodes comprised four electrodes placed on the abdomen, an abdominal reference electrode placed above the *pubic symphysis* and a common mode reference electrode (with active-ground signal) placed on the left leg [39], [103].

Although the database includes a total of 12 recordings, we only used 8 of them for the experiments. The reason is that the quality of some of the recordings (r04, r07, r11, and r12) is low for the needs of morphological analysis. Fig. 2 shows the examples of the omitted abdominal signals along with the estimated fECG signals. It can be noticed that the extraction system was not able to suppress the unwanted signals and thus the resulting fECG signals are too noisy for the needs of any further analysis. In fact, even accuracy of the fHR determination is quite low in comparison with the rest of the dataset as demonstrated by the fHR traces displayed in Fig. 3 and other investigations presented in [30], [104].

Reference annotations are available at ADFECGDB to compare the accuracy of determining the R peak positions

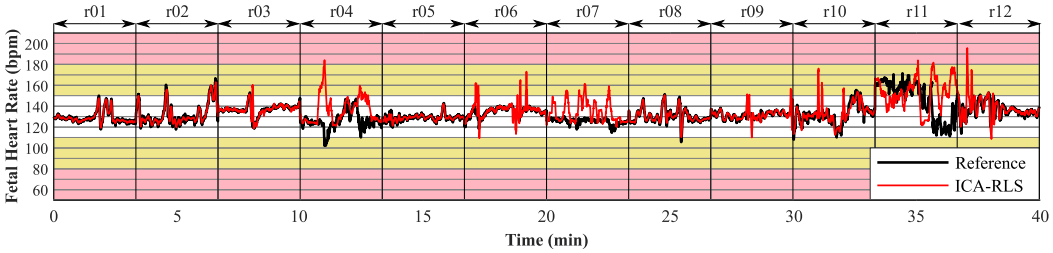

FIGURE 3. Examples of the fHR traces estimated using the omitted recordings (r04, r07, r11, and r12) to demonstrate their low quality for the purpose of morphological analysis.

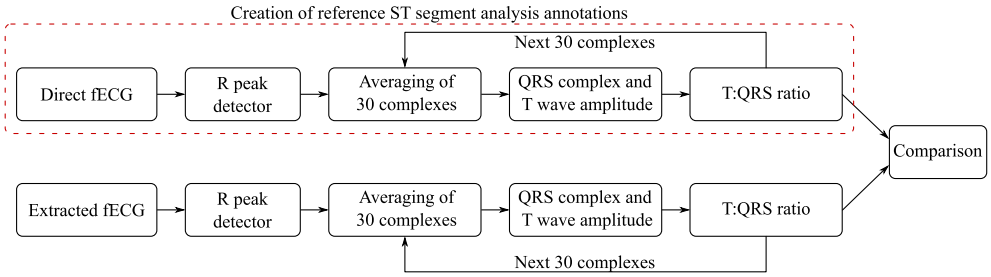

FIGURE 4. Block diagram of ST analysis using reference and extracted fECG signal.

in the extracted signal with respect to the reference. In this study, however, we focus on morphological analysis, for which no reference values or annotations are available for possible comparison. For this reason, we had to create reference annotations for each record. Fig. 4 illustrates the process of generating ST analysis reference values from the fECG signal measured by the scalp electrode (direct fECG) and estimated ST analysis values using the extracted fECG signal. These annotations are available at https://dx.doi.org/10.21227/70cd-bw64 [105].

B. HYBRID SYSTEM DESIGN

The hybrid system is designed to perform ST segment analysis from extracted fECG signals using a combination of FastICA and RLS algorithms, which allows us to combine the advantages of both methods and achieve more accurate fECG extraction. Fig. 5 shows schematic diagram of the experimental setup with examples of the outputs. The system is based on our previous research focused on fHR estimation introduced in [29], [30]. The process comprises of following steps:

- *Selection of suitable aECG signals* - Table 4 shows the RLS filter order settings for each record as well as selected electrode combination used as the ICA-RLS hybrid system input. Filter order settings and selected electrode combination was based on the previous study [29] focused on the selection of suitable electrodes and RLS filter order for each recording.
- *Preprocessing* - bandpass finite impulse response filter (FIR) with cut-off frequencies 3 and 150 Hz, filter order of 500.
- *Decomposition of the signal using FastICA* - the algorithm decomposes the input signals to multiple independent components including mECG* which is a component corresponding to the maternal mECG, and aECG*, which is a component corresponding to the aECG inputs with an enhanced fetal component. The FastICA algorithm is set to at least 20 iterations and 3 output components.
- *Adaptive filtering* - the estimated mECG* and aECG* signals are used as reference and primary inputs to the RLS algorithm, respectively. For the RLS algorithm, the forgetting factor was set to 1 and the filter order varied in the range from 1 to 100. Using this adaptive algorithm, the fECG signal was extracted. Table 4 shows the RLS filter order settings for each recording as well as selected electrode combination used as the ICA-RLS hybrid system input.

The estimated fECG signal enters the R peak detector based on continuous wavelet transform (CWT) [29], [106]–[108]. This detector estimates the positions of R peaks that will be subsequently compared with the reference annotations obtained using the direct signal registered with a help of FSE (see Fig. 5). This signal is pre-processed by the FIR filter described above. For the recordings from ADFECGDB database (accessible at Physionet) the annotations were available, for the remaining signals the R peak positions were determined using the CWT-based detector.

The instantaneous fHR was estimated using the determined intervals between consecutive R peaks (RR intervals). Subsequently, the fHR traces for both reference and estimated signals were determined and compared using the

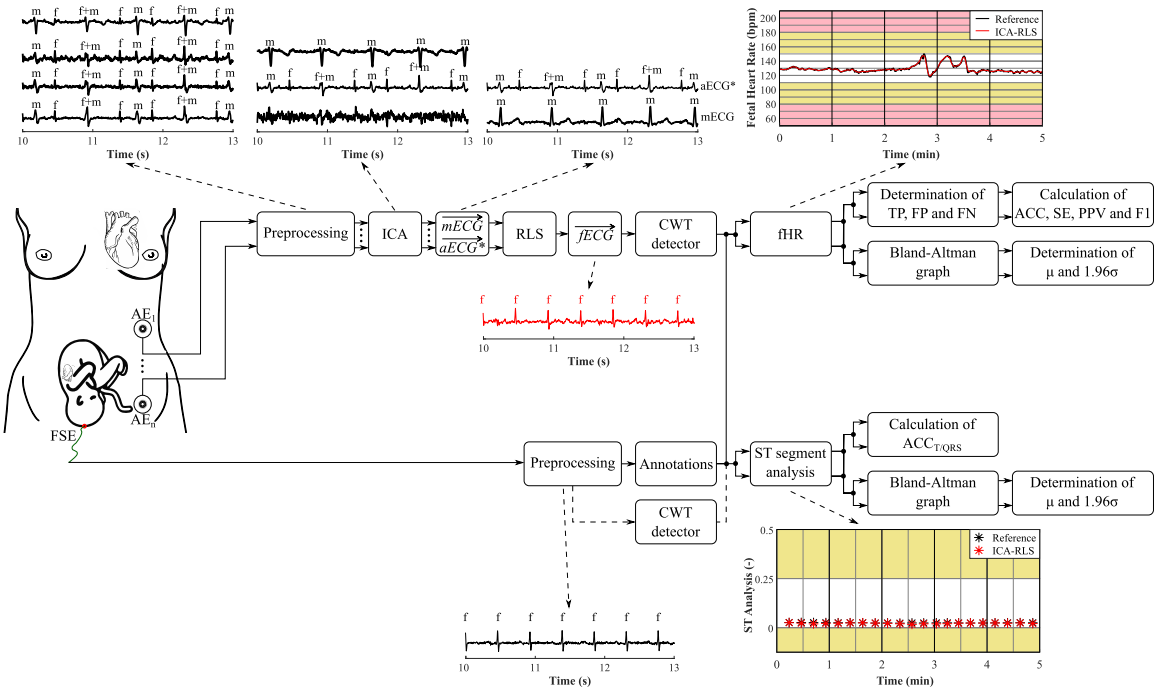

FIGURE 5. Example of the STAN monitor output: (a) fHR trace, (b) uterine contractions (toco), (c) T/QRS trace, and (d) example of the averaged T/QRS.

TABLE 4. ICA-RLS algorithm settings.

Recordings	r01	r02	r03	r05	r06	r08	r09	r10
Combination of electrodes	1,3,4	1,2,3,4	2,4	1,4	3,4	1,4	1,4	1,4
Filter order	4	66	52	34	16	100	16	56

Bland-Altman plot. The Bland-Altman plot shows the mean value μ and $\pm 1.96\sigma$, which reflect the difference between the estimated and reference fHR traces. Moreover, the R peak positions were used to evaluate the quality of the extraction based one the ACC, SE, PPV and F1 indices defined by (1), (2), (3), and (5), respectively. The true positive (TP), false positive (FP), and false negative (FN) values were determined using the estimated and reference signals. The time interval for the TP determination was selected as ± 50 ms from the reference R peak [29], [32].

$$ACC = \frac{TP}{TP + FP + FN} \cdot 100\,(\%), \tag{1}$$

$$Se = \frac{TP}{TP + FN} \cdot 100\,(\%), \tag{2}$$

$$PPV = \frac{TP}{TP + FP} \cdot 100\,(\%), \tag{3}$$

$$F1 = 2 \cdot \frac{Se \cdot PPV}{Se + PPV} = \frac{2 \cdot TP}{2 \cdot TP + FP + FN} \cdot 100\,(\%). \tag{4}$$

Finally, the main parameter to evaluate the quality of the extraction, being the main goal of this study, was based on the applicability of the ST segment analysis on the estimated fECG signal. The individual fQRS complexes and the determined T/QRS are displayed in the graph to compare the efficacy for visual evaluation. The objective evaluation of the determined T/QRS is performed using the $ACC_{T/QRS}$ parameter. For detailed description of the ST segment analysis, please refer to the next Section.

C. ST SEGMENT ANALYSIS

In the clinical practice, the STAN machine calculates the normal T/QRS ratio for each fetus and thus establishes the '*baseline value*' over the first 4–5 minutes [109]. The device then analyses every 30 ECG complexes and compares them with this '*baseline value*'. Each analysis is marked on the fHR trace with a cross '*X*' (see Fig. 1) or star '*' (see Fig. 6). If the analyzed ECG complexes differ significantly from the '*baseline value*', they will be flagged up as an '*ST event*'. In the presence of an '*ST event*', it is necessary to classify the CTG trace according to STAN guidelines (see Table 3) and then to determine whether it is significant and requires any action [109].

In our study, we first applied the R peak detection and then carried out the analysis of 30 averaged consecutive fECG cycles. For averaging, we determined a window with a

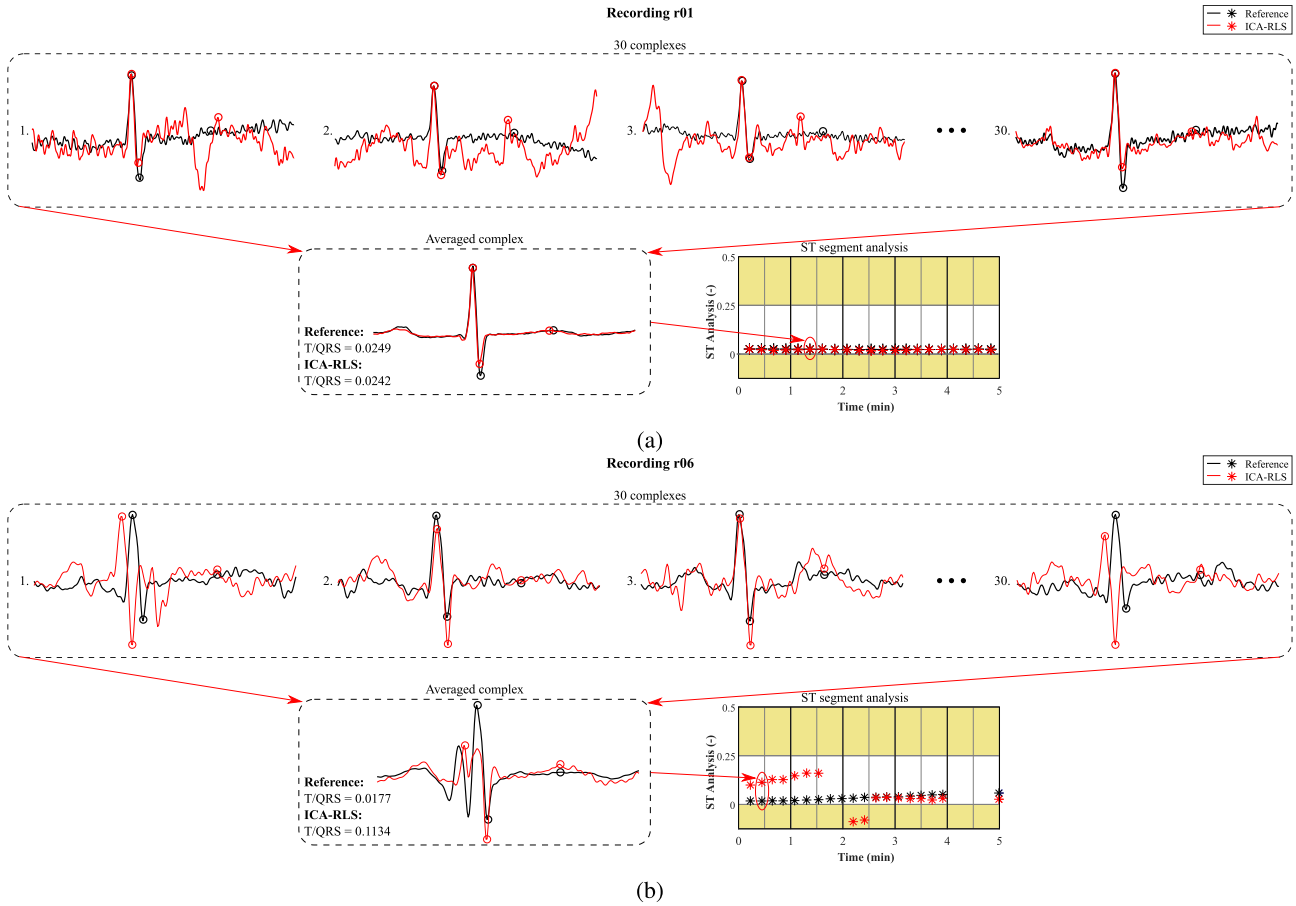

FIGURE 6. Example of the averaging and T/QRS calculation for NI- ST-analysis: (a) recording r03, high accuracy achieved, and (b) recording r06, low accuracy achieved.

fixed length of 600 ms (beginning 190 ms before the R peak location and ending 410 ms after it) to cover all the physiological changes in the fECG cycle. Fig. 6 shows examples of the averaging and T/QRS calculation procedure for signals providing good (Fig. 6a) and poor results (Fig. 6b).

When assessing the quality of T/QRS estimation, we take into account the amplitude of the R peaks, S peaks, and T waves. When pre-processing signals, the magnitude of the signal is normalized (according to the R peak amplitude) to prevent an error caused by poor signal amplification. First, it is necessary to determine the beginning and the end of the QRS complex. These are calculated using the wavelet transform with first order Gaussian wavelet base and 4 levels of decomposition, similarly as in the R peak detection.

For T-wave detection, the wavelet-based detector was not efficient enough even when using different types of waves and decomposition levels, probably due to its low amplitude in fECG signals. The T wave detection was thus realized based on the approach presented in [110]. For this purpose, the signal was first duplicated and a Butterworth bandpass filter was applied at frequency band of 0.5–10 Hz, which is believed to cover most of the T wave content [110]. Subsequently, the QRS complex was suppressed and the T wave was detected by using thresholding. Finally, ST analysis was performed by calculating the T:QRS ratio for each of the averaged fECG cycle, i.e. the ratio between the T wave amplitude and peak-to-peak amplitude the QRS complex.

The ability of the hybrid system to extract the fECG signal of a sufficient quality for the purpose of the morphological analysis of the fECG signal was assessed by the parameter called *T/QRS Accuracy* (denoted as $ACC_{\mathrm{T/QRS}}$). The definition of $ACC_{\mathrm{T/QRS}}$ was inspired by a study presented in [1] and can be described by the following formula (5):

$$ACC_{\mathrm{T/QRS}} = \left(1 - \frac{|T/QRS_{\mathrm{REF}} - T/QRS_{\mathrm{FILTER}}|}{T/QRS_{\mathrm{REF}}}\right) \cdot 100\ (\%), \tag{5}$$

where T/QRS_{FILTER} is the T:QRS ratio calculated for the averaged complexes being the result of the analysis of the extracted signals, and T/QRS_{REF} is the reference T:QRS ratio calculated for the averaged complexes determined based on the analysis of the direct signal from the scalp electrode.

D. ECG SIGNAL FEATURE EXTRACTION

Several approaches to detect the individual features of the ECG waveform were presented in the literature, which can also be used for the purposes of non-invasive fetal ST analysis:

- A simple method introduced in 1985 known as the Pan and Tompkins detector has been often used to detect R peaks [111]. As an example the work [112] can be given, where based on signals from the MIT/BIH database [113] the detection accuracy reached 99.00%. An improved variant of the algorithm was also tested in [114] on MIT/BIH and the sensitivity of the method was 99.40%.
- For noisy signals, more robust detection algorithms should be used. Wavelet transform is a prevalent method for the QRS complex detection. When using this method, the wavelet base needs to be selected carefully. *Mexican hat, symlet, morlet, Daubechies* and the first derivative of the Gaussian function are among the most frequently used base functions for the detection of QRS complexes. In [115], the authors present the use of the *db1* wavelet to detect the R peak on a scale of 1 and to detect the P and T waves on scales 4 and 5. In [116], the authors use the *db4* waveform to detect QRS complexes. Using the MIT/BIH database the results with sensitivity of 98.10% were obtained. For further details on this method and its application please refer to [106], [117].
- Similar thresholding-based detector can be used to detect P and T waves in high-quality signals. This algorithm was tested in [118], where the authors aimed to estimate the beginnings and ends of these waves. However, according to the authors, this method is not very suitable for automated evaluation of P and T wave localization.
- In [110], the authors presented a method for T wave detection. The algorithm consists of the following steps: preprocessing (0.5–10 Hz bandpass filtering), QRS complex suppression, generation of the so-called potential blocks by using moving averages, and thresholding as the final step. The algorithm was tested on both the MIT/BIH database [113] and the QT database [119], on average a sensitivity of over 98.50% was achieved for both datasets.
- In [120], the authors use *quadratic spline-wavelet*, applied to the region starting 0.25·R-R before the R peak to detect the P wave. The algorithm was tested on a QT database [119] with an accuracy of 99.90%.
- In [121], the authors present the detection of P wave and T wave by the method of particle swarm optimization. The method is also suitable for detecting the beginnings and ends of waves. The authors performed the evaluation on the QT database and the examined indices of the detection quality (sensitivity and positive predictive value) exceeded 95.00%.
- In [122] the author presents the possibility of detecting both P wave and T wave by continuous wavelet transform and Gaussian wavelet. Because these waves do not have as steep a course as the QRS complex, a scale of 4 is more suitable for them. For P wave detection, the window is located between the end of the previous T wave and the beginning of the QRS complex. In addition, this method makes it possible to detect biphasic waves.
- In [123], the authors compared the methods for detecting the end of a T wave:
  - The Philips method represents the construction of a line connecting the top of a T wave and a point 100 ms behind the inflection point of the falling edge of the wave. At the point of the highest value of the difference between the line and the signal, the end of the T-wave is located.
  - The derivation method consists of deriving the signal and finding the first extreme of the derivative behind the T-wave.
  - MS-Tpeak method proposes the connection of the top of the T wave and the inflection point. At the point where the line thus formed intersects the signal, the end of the T-wave is determined.
  - The tangent interpolation method is based on the interpolation of an inflection point by a tangent. At the point where the tangent intersects the isoline obtained from the TP interval, the end of the T wave is determined.

To perform ST analysis, it is necessary to determine the amplitude of R peaks, S peaks and T waves. A detector based on a CWT was used to detect the positions of the R peaks. First, the signal decomposition is performed by CWT using Gaussian mother wavelet and 5 levels of decomposition. Subsequently, all local maxima and minima with a minimum distance of 0.2 s are found. The maximum threshold is set to $0.4 \cdot A_{max}$, where A_{max} is the local maximum of the highest amplitude in the first 4 s of the signal. The minimum threshold is set to $0.4 \cdot A_{min}$, where A_{min} is the local minimum of the highest amplitude in the first 4 s of the signal. This maximum and minimum threshold is then adjusted accordingly when shifted through the signal. In the next step, all local maxima exceeding the set maximum threshold are marked as the modulus maxima. Similarly, all local minima exceeding a specified minimum threshold are marked as the modulus minima. In the last step of R peak detection, the areas where the distance between the recorded modulus minima and the modulus maxima is less than 120 ms (maximal length of the QRS complex) are determined and the centers between them are referred to as zero-crossing. Finally, the largest values are found in the zero-crossing region in order to determine the positions and amplitudes of the R peaks.

The QRS complexes are cut out according to the determined R-positions; averaging of 30 QRS complexes is performed. The position of the T wave is determined in following steps and explained on one averaged complex as illustrated in Fig. 7:

1) DWT with db6 Daubechies wavelet and decomposition level 7 is applied to averaged complex; complex is then reconstructed using the wavelet (detail) coefficients at level 7. The algorithm then detects all local maxima

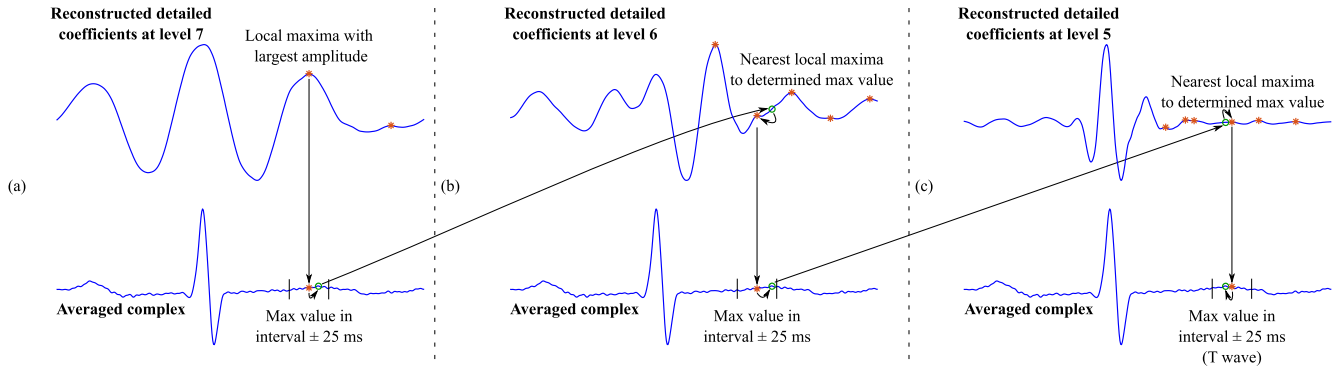

FIGURE 7. Illustration of the T wave detection process.

after determined R peak position. The local maximum with the largest amplitude is determined (Fig. 7(a)) and its position is used to find the approximate T wave position, which is selected as the highest value detected within ±25 ms from this position in averaged complex.

2) Averaged complex after decomposition from step a) is reconstructed using the wavelet (detail) coefficients at level 6. The algorithm then detects all local maxima after determined R peak position. The nearest local maximum to the estimated approximate T wave position is determined (Fig. 7(b)) and its position is used to find the approximate T wave position, which is selected as the highest value detected within ±25 ms from this position in averaged complexes.
3) Averaged complex after decomposition from step a) is reconstructed using the wavelet (detail) coefficients at level 5. The algorithm then detects all local maxima after determined R peak position. The nearest local maximum to estimated approximate T wave position is determined (Fig. 7(c)) and its position is used to find the approximate T wave position, which is selected as the highest values detected within ±25 ms from this position in averaged complex.

Finally, to determine the amplitude of the S peak, the lowest value in the interval between the detected R peak and the following 40 ms is determined. This is done for all averaged complexes.

IV. RESULTS

For statistical evaluation of the fHR estimation, TP, FP and FN values were determined and used to calculate the quality indices such as ACC, SE, PPV, and F1, see Table 5. The results presented in Table 5 show that the ICA-RLS method achieved high efficacy in fHR estimation. The accuracy (ACC) of over 95% was achieved for the recordings r01, r02, r05, r08 and r09, while for the recordings r01, r02, r03, r05, r08, r09 and r10 the sensitivity (SE) of over 95% was attained. Finally, the PPV and F1 values above 95% were noted for the recordings r01, r02, r03, r05, r08, and r09. Moreover, very low FP a FN values were obtained while analyzing the recordings r01, r05, and r08. Moreover, Table 5 includes the results of ICA-RLS-EMD and ICA-RLS-WT methods. These results show that ICA-RLS method achieves lower accuracy for some recordings due to the absence of the application of EMD or WT method in the last step due to their negative effect on the signal morphology.

The parameter $ACC_{\mathrm{T/QRS}}$ was used for statistical evaluation of the method ability to recover the signal of sufficient quality for the morphological analysis. The evaluation was carried out for groups of averaged complexes as listed in Table 6. The results demonstrate functionality of the method for the ST segment analysis on 7 out of 8 recordings. For the recordings r01, r02, r05, r08, r09, and r10 it was possible to perform the ST analysis for the entire length of the recordings. The most accurate results were obtained for the recordings r01, r02, and r08, while for the recordings r05, r09 and r10 the accuracy level was high enough ($ACC_{\mathrm{T/QRS}} > 54.84\%$). For the recording r06, it was possible to achieve high quality only for a part of the signal. Unfortunately, for the recording r03 the ST segment analysis was not functional due to poor quality of the input signal.

Fig. 8 shows examples of the averaged fQRS complexes obtained using the proposed hybrid ICA-RLS method in comparison with the reference fQRS complexes obtained using the fetal scalp electrode for the recording r01. This recording was selected since it achieved the best results of the ST analysis. This example demonstrates that the choice of the hybrid method and its settings are appropriate since they provide estimated signal of high-quality and do not affect its morphology. It should be noted that the quality of the input aECG signals plays an important role in fECG signal extraction and non-invasive ST segment analysis. If the morphology of the input abdominal signal is distorted due to poor quality of the registration itself (as is the case of recording r03), it is nearly impossible to estimate signal of a sufficient quality to perform non-invasive ST segment analysis.

As the common technique to evaluate two methods of measurement is the Bland-Altman plot, we used it to assess the accuracy of the proposed hybrid extraction procedure. We compared our results with the reference annotations and

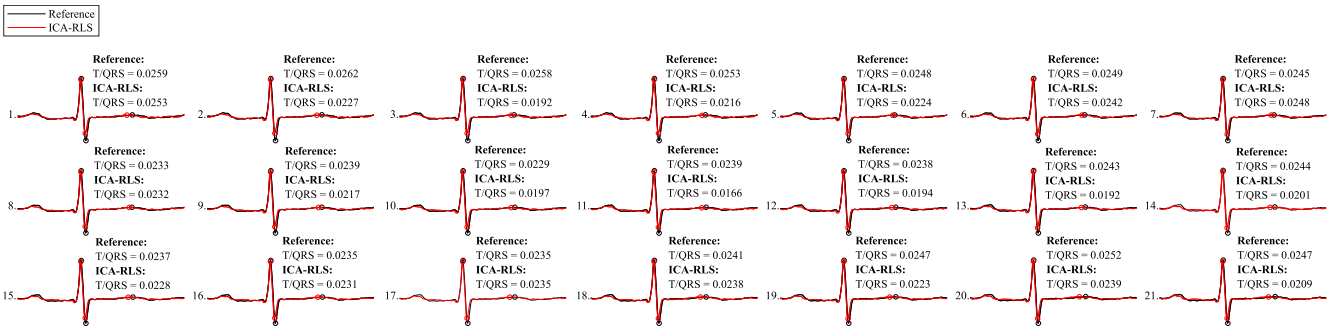

FIGURE 8. Comparison of the averaged T/QRS estimated using the hybrid method ICA-RLS in comparison with the reference T/QRS obtained by means of fetal scalp electrode (the recording r01).

TABLE 5. Statistical evaluation of the fHR determination in signal obtained by the ICA-RLS, the ICA-RLS-EMD and the ICA-RLS-WT method.

ICA-RLS								
Recordings	**Beats**	**TP**	**FP**	**FN**	**ACC (%)**	**SE (%)**	**PPV (%)**	**F1 (%)**
r01	644	643	4	1	99.23	99.85	99.38	99.61
r02	660	653	11	7	97.32	98.94	98.34	98.64
r03	684	669	22	15	94.76	97.81	96.82	97.31
r05	645	644	5	1	99.08	99.85	99.23	99.54
r06	674	623	66	51	84.19	92.43	90.42	91.42
r08	651	649	2	2	99.39	99.69	99.69	99.69
r09	657	645	5	12	97.43	98.17	99.23	98.70
r10	637	623	58	14	89.64	97.80	91.48	94.54
ICA-RLS-EMD								
Recordings	**Beats**	**TP**	**FP**	**FN**	**ACC (%)**	**SE (%)**	**PPV (%)**	**F1 (%)**
r01	644	642	1	2	99.53	99.69	99.84	99.76
r02	660	658	1	2	99.55	99.70	99.85	99.77
r03	684	677	2	7	98.69	98.98	99.71	99.34
r05	645	643	0	2	99.69	99.69	100.00	99.84
r06	674	630	27	44	89.87	93.47	95.89	94.66
r08	651	650	1	1	99.69	99.85	99.85	99.85
r09	657	652	0	5	99.24	99.24	100.00	99.62
r10	637	617	33	20	92.09	96.86	94.92	95.88
ICA-RLS-WT								
Recordings	**Beats**	**TP**	**FP**	**FN**	**ACC (%)**	**SE (%)**	**PPV (%)**	**F1 (%)**
r01	644	643	1	1	99.69	99.85	99.85	99.85
r02	660	656	1	4	99.24	99.39	99.85	99.62
r03	684	647	4	37	94.04	94.59	99.39	96.93
r05	645	644	1	1	99.69	99.85	99.85	99.85
r06	674	592	43	82	82.57	87.83	93.23	90.45
r08	651	650	1	1	99.69	99.85	99.85	99.85
r09	657	626	1	31	95.14	95.28	99.84	97.51
r10	637	626	33	11	93.43	98.27	94.99	96.61

direct signals. However, some annotations contained several outliers that affected the determination of mean μ and 1.96σ values when plotting the Bland-Altman graph. These outliers were replaced with the annotations calculated as the mean of the preceding and consecutive correctly determined values.

Table 7 shows mean values of μ and $\pm 1.96\sigma$ allowing for assessing the ability of ICA-RLS method to estimate the signal of suitable quality for fHR and ST analysis. The closer the values of μ and $\pm 1.96\sigma$ are to zero, the smaller is the difference between the extracted and the reference signals. In the case of fHR determination, low values demonstrating the effectiveness of the method, were achieved for the recordings r01, r02, r03, r05, r08, and r09. Higher values of both parameters were obtained for the recordings r06

TABLE 6. Evaluation of the applicability of the ICA-RLS method for ST analysis according to $ACC_{T/QRS}$ (%).

Order of T/QRS	Recordings							
	r01	r02	r03	r05	r06	r08	r09	r10
1	97.7	96.9	17.91	73.9	< 1.00	74.26	85.92	75.51
2	86.65	94.12	< 1.00	66.48	< 1.00	76.12	78.57	83.49
3	74.41	82.55	< 1.00	48.62	< 1.00	70.31	74.8	84.83
4	85.41	70.5	< 1.00	56.75	< 1.00	73.06	78.65	72.81
5	90.14	93.13	< 1.00	50.79	< 1.00	77.13	73.96	59.64
6	97.34	94.42	< 1.00	45	< 1.00	73.43	94.34	60.53
7	98.88	84.43	< 1.00	46.59	< 1.00	74.45	93.48	62.75
8	99.49	77.61	< 1.00	39.2	< 1.00	80.4	93.62	59.6
9	91.03	73.68	< 1.00	44.78	< 1.00	86.82	70.29	55.76
10	85.84	88.15	< 1.00	53.24	< 1.00	91.94	52.72	77.84
11	69.44	98.8	< 1.00	65.48	< 1.00	95.13	35.71	59.6
12	81.62	93.78	< 1.00	66.27	90.67	93.11	41.27	40.17
13	78.8	94.5	< 1.00	72.82	93.52	90.58	54.52	33.83
14	82.54	99.13	< 1.00	85.96	84.99	92.3	30.85	32.97
15	95.93	81.16	< 1.00	60.63	70.13	87.8	4.03	29.88
16	98.57	69.72	< 1.00	63.23	63.56	88.49	20.23	25.03
17	99.88	60.98	< 1.00	64.91	46.65	89.44	27.69	8.07
18	98.53	44.57	< 1.00	76.22	61.37	94.29	32.86	18.7
19	90.26	40.91	< 1.00	78.77	45.5	98.26	—	6.6
20	94.79	54.58	< 1.00	74.9	—	97.76	—	—
21	84.33	10.77	< 1.00	89.95	—	96.97	—	—
22	—	40.98	—	95.18	—	99.48	—	—

TABLE 7. Mean values μ and $\pm 1.96\sigma$ determined for ICA-RLS, ICA-RLS-EMD and ICA-RLS-WT in fHR and ST analysis.

Record	ICA-RLS				ICA-RLS-EMD				ICA-RLS-WT			
	fHR		ST analysis		fHR		ST analysis		fHR		ST analysis	
	μ (bpm)	$\pm 1.96\sigma$ (bpm)	μ (bpm)	$\pm 1.96\sigma$ (bpm)	μ (bpm)	$\pm 1.96\sigma$ (bpm)	μ (bpm)	$\pm 1.96\sigma$ (bpm)	μ (bpm)	$\pm 1.96\sigma$ (bpm)	μ (bpm)	$\pm 1.96\sigma$ (bpm)
r01	0.01	1.76	-0.0025	0.0043	-0.25	5.39	-0.0082	0.0061	0.01	1.64	0.0030	0.0087
r02	-0.31	5.09	0.0042	0.0072	-0.22	7.63	0.0357	0.0264	0.03	3.06	-0.0130	0.0111
r03	0.11	5.83	0.0307	0.0102	-0.26	2.91	0.0165	0.0068	0.12	5.31	-0.0111	0.0093
r05	0.02	2.07	0.0063	0.0046	-0.13	4.13	-0.0034	0.0038	0.01	1.91	-0.0123	0.0052
r06	1.29	14.08	0.0060	0.1942	-1.15	5.62	1.7625	2.4839	0.27	10.40	1.3922	3.7476
r08	0.01	1.91	-0.0037	0.0055	-0.26	7.12	-0.0146	0.0093	0.02	1.91	0.0006	0.0030
r09	0.09	2.01	0.0086	0.0112	-0.48	3.60	0.0229	0.0196	-0.08	4.19	-0.0063	0.0058
r10	1.39	13.65	0.0134	0.0137	-0.32	8.73	1.7567	2.9646	0.11	7.81	0.0308	0.0289

and r10, which means that for these recordings the fHR was not extracted as accurately. In the case of ST analysis, low values, and thus high effectivity, were achieved for the recordings r01, r02, r05, r06, r08, and r09. However, for recordings r06 and r09, a higher value of $\pm 1.96\sigma$ was achieved, which corresponds to lower efficacy of ST analysis. Similarly, for the recordings r03 and r10 we obtained high values of both parameters as well. Moreover, Table 7 includes mean values of μ and $\pm 1.96\sigma$ for ICA-RLS-EMD a ICA-RLS-WT methods for fHR determination and ST analysis. Below we provide 3 examples of Bland-Altman plots: Fig. 9 and Fig. 10 present cases of the method efficiency for both fHR and ST analysis, whereas Fig. 11 shows an example of accurate determination of fHR and ineffective ST analysis.

Finally, we provide a graphical illustration of the fHR traces and ST analysis as displayed by the STAN monitor screen and compare the estimated parameters with the reference ones. Fig. 12 shows such traces for all tested recordings. The upper waveform represents fHR traces obtained by the ICA-RLS method (red) along with the reference fHR trace (black) created using the database annotations. The lower part shows the results of the ST analysis. The T:QRS ratios obtained by the ICA-RLS method (red stars) are again compared with the T:QRS ratios determined using the reference signal.

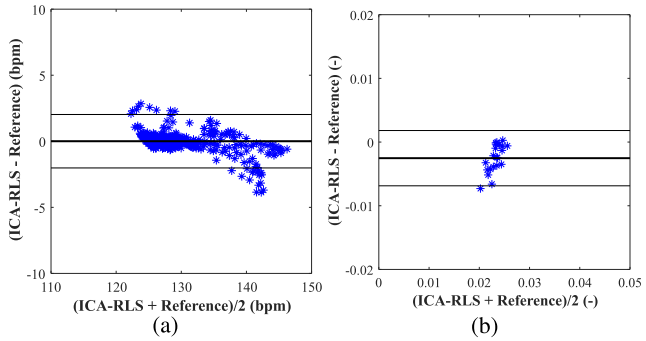

FIGURE 9. Bland-Altman plots for the comparison of the parameters obtained using the reference and estimated signals for the recording r01: (a) fHR, and (b) ST analysis.

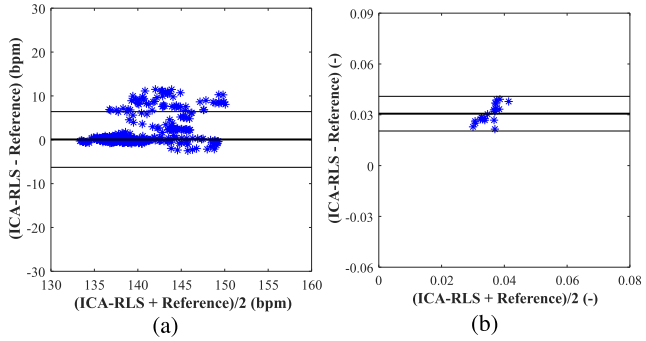

FIGURE 10. Bland-Altman plots for the comparison of the parameters obtained using the reference and estimated signals for the recording r03: (a) fHR, and b) ST analysis.

The more the estimated fHR traces and T:QRS ratios follow the reference trends, the more efficient is the method of the fECG extraction. It can be stated that our method allowed for high accuracy fHR monitoring in case of all tested signals, especially for the recordings r01, r02, r05, r08 and r09, where the estimated fHR trace follows perfectly the trend of the reference one. Nevertheless, for the recordings r03, r06, and r10 slight deviations from the reference fHR trace can be noticed. However, these are negligible differences that do not affect the final diagnosis of the fetal distress.

Furthermore, it can be stated that the ST analysis was successful for the recordings r01, r02, r05, and r08. While for the recordings r09 and r10 slight deviations of the T:QRS ratios from the reference can be seen. Again, these differences would not affect the final fetal diagnosis. When investigating the recordings r06, we noticed that most part of it was analyzed accurately, however with slight deviations caused by a poor quality of the original aECG signal. The worst results were achieved for the recording r03, where the quality of the estimated signal was not suitable for the ST analysis and thus the analysis was not performed.

V. DISCUSSION

The results of our experiments show that the proposed hybrid method combining the ICA and RLS algorithms is able to extract a high quality fECG signal and accurately determine

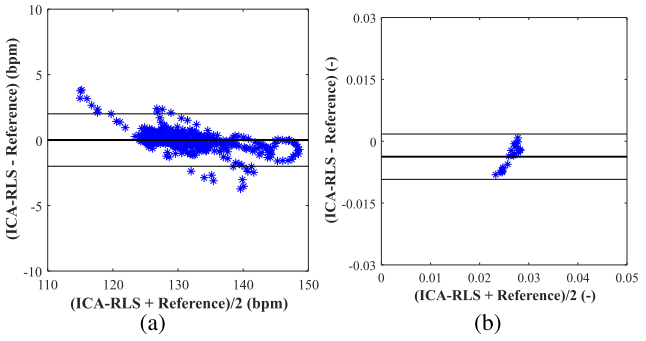

FIGURE 11. Bland-Altman plots for the comparison of the parameters obtained using the reference and estimated signals for the recording r08: (a) fHR, and (b) ST analysis.

the fHR for all tested recordings. However, the primary objective of the study was to perform the ST segment analysis in order to access equivalent diagnostic information to the one obtained using the invasive monitoring. This has been proven as possible, but compared to the fHR determination much more attention must be given to the selection of appropriate filtering methods and their settings. Also, suitable detection methods must be chosen and high-quality input aECG recordings must be used in order to automatically extract a fECG signal of sufficient quality.

To illustrate the effect of the filtration method used on the estimated signal, we compared the averaged fQRS complexes extracted using the hybrid method ICA-RLS, the ICA-RLS-EMD and the ICA-RLS-WT, see Fig. 13. This figure shows the negative effect of the EMD and the WT method on the resulting signal morphology. In terms of detection of R peaks and determination of fHR, these methods are very effective. However, the EMD based method and the WT based method are not suitable for ST segment analysis because it changes the fECG signal morphology. These changes can be noticed in all elements of the PQRST complex, except for the R peak, which could affect ST analysis and lead to loss of valuable clinical information that could otherwise be obtained from NI-fECG. The most significant changes occur in the P and Q wave. The S and T waves are affected less significantly, but even such differences have a great impact on the accuracy of ST analysis and the loss of valuable clinical information that would be otherwise obtained from NI-fECG.

Furthermore, to illustrate the influence of the quality of aECG signals on the efficiency of the fECG extraction and the subsequent ST analysis, we present an example of results of ST analysis performed on both estimated and reference signals for all of the tested recordings (see Fig. 14). Six parts of the trace were selected to show instances of the inputs, estimated signals and direct fECG signal from fetal scalp. Three of these selected samples, denoted as (a), (b), and (c), correspond to the sections where an accurate ST analysis was achieved (the estimated T:QRS ratio is in the accordance with the reference one). For each example, we provide 5-second fragments of signals corresponding to that particular time

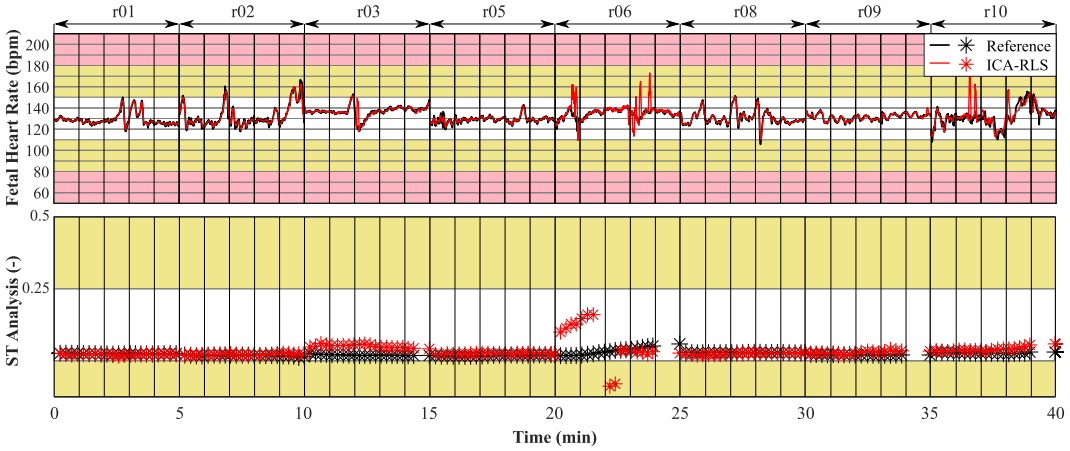

FIGURE 12. Graphical illustration of the fHR traces and ST analysis as displayed by the STAN monitor.

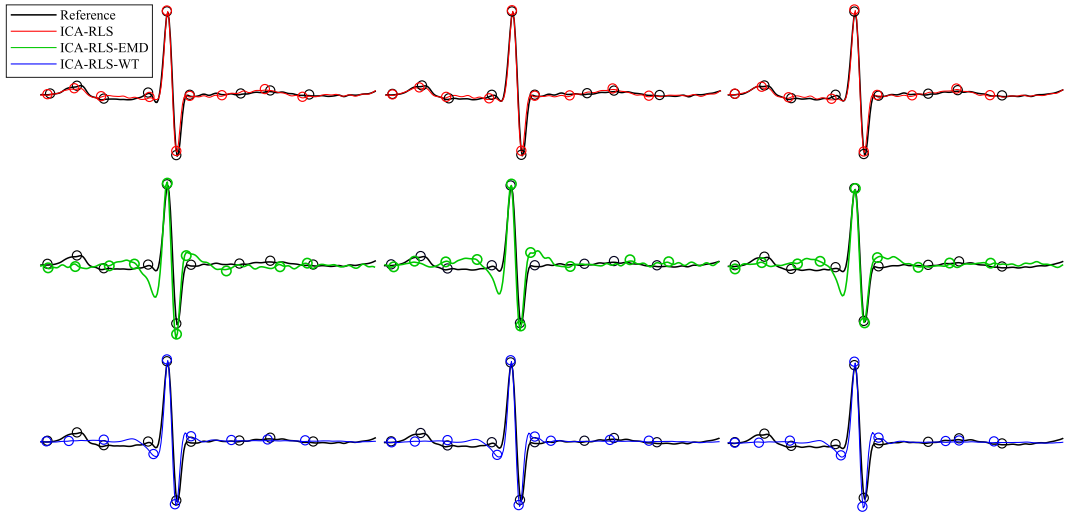

FIGURE 13. Comparison of averaged fQRS complexes obtained using hybrid extraction system ICA-RLS, ICA-RLS-EMD and ICA-RLS-WT on the recording r05 illustrating the drawback of WT method used in postprocessing of the resulting fECG signal.

frame. It can be noticed that the quality of the extracted fECG is high and thus the ST analysis could be performed. The rest of the examples, denoted as (d), (e), and (f), correspond to the sections of the signal where the determination of the ST analysis was not successful (the estimated and reference T:QRS ratio differ). The quality of the aECG and consequently the extracted fECG signals is poor compared to the previous cases. The signal contains maternal residua and its morphology is deformed, hence, the ST segment analysis was not successful.

Finally, we compared the results obtained with the results of a very few studies that have dealt with the morphological analysis of the fECG signal (these are summarized in Table 8). Objective comparison of results is very difficult since the authors use different databases for testing (the Non-Invasive Fetal ECG Arrhythmia Database [46], the Fetal ECG Synthetic Generator [38], use their own synthetically generated signals [1] or used their own real signals [20]. It is clear that most authors use synthetic data for experiments, on which they achieve very accurate results. Unfortunately, subsequent testing of algorithms on real data usually achieves significantly worse results.

Herein, we used real records for our experiments containing a signal from the scalp electrode, which we used to create annotations to determine the accuracy of ST analysis. For future research in this area, it would be appropriate test the algorithms on more extensive dataset with continuously recorded abdominal direct ECG recordings. Another limitation in objective comparison is the use of various parameters (coefficient of determination [44] or the root mean square error [48]) to evaluate the effectiveness of morphological analysis. For these reasons, we tried to make a combination of both objective and subjective comparison of the achieved results.

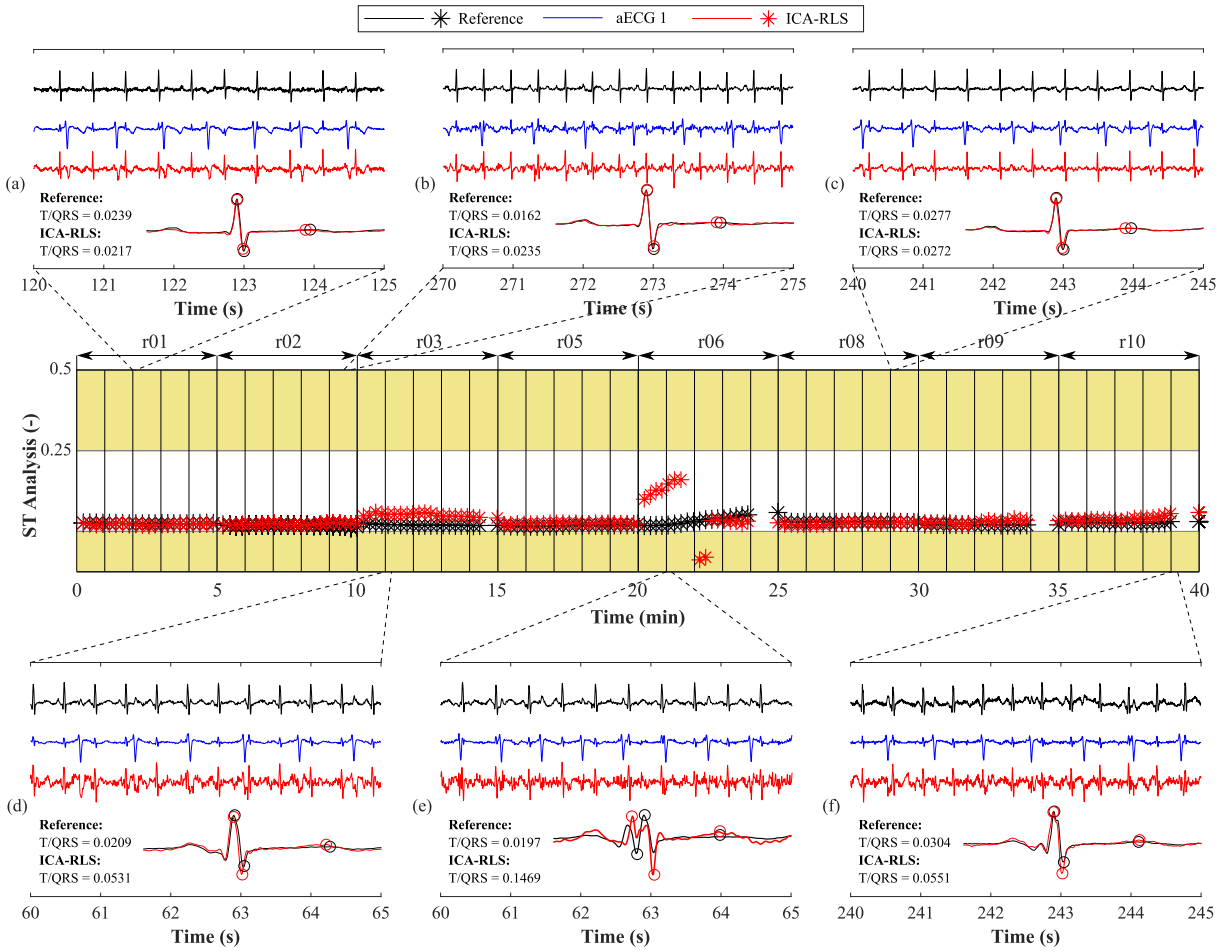

FIGURE 14. Example of the ST segment analysis performed on the fECG signal obtained by the ICA-RLS hybrid method. Subfigures (a), (b), and (c) show 3 sections where the accuracy of ST analysis was high, while (d), (e) and (f) show 3 sections of inaccurate ST segment analysis.

- In [45], optimal shrinkage was used to determine fHR with accuracy of 79.25 ± 31.75% for (semi)-real records and with 93.21 ± 14.31% for synthetic records. In both cases, these are worse results than we have achieved. In case of morphological analysis, the authors did not deal with ST analysis, but with P wave and T wave detection, in which they reached values of 4.85 ± 8.33 and 0.22±0.34 according to the normalized mean amplitude error. The authors state that the method was also effective for recordings containing arrhythmias, but less effective for signals with significant mECG amplitude.
- The authors in [46] dealt with the detection of arrhythmias by analyzing the morphology of the P wave. The authors used their own real records acquired on 500 women (gestational age: 22–41 weeks) for testing. The study does not report statistical results for the determination of fHR or for the analysis of P wave morphology. However, the authors state that the algorithm was able to detect all cases of arrhythmias and in only one case was the arrhythmia incorrectly identified due to the low resolution of the P wave.
- Three types of methods (BSS methods, TS and adaptive methods) were tested in [44]. When determining fHR, the algorithms achieved an accuracy of 86.40–99.90%, 77.40–96.00%, and 87.1–97.90%, respectively. In all cases, these are slightly worse results than those obtained using the algorithm presented by us. The authors also dealt with determining the QT interval and the T/QRS ratio. The evaluation was performed using the coefficient of determination, which reached the values of 0.189, 0.846, and 0.574, respectively, when evaluating the accuracy of the estimated QT interval, and 0.098, 0.916, and 0.812, respectively, when determining the T/QRS ratio. The least accurate results were obtained with records containing ectopic beats.
- In [47], the authors did not deal with the determination of fHR, but only with the determination of the accuracy of the estimated length of the QT interval using extended Kalman filter. They managed to achieve an accuracy of 4.00 ms evaluated by the median absolute error. The advantage of this method is that it requires only single-channel as an input.

TABLE 8. Summary of state-of-the-art methods for NI-fECG morphological analysis.

Author, source	Algorithm	fHR (%)	Morphological Analysis	Evaluation of Morphological Analysis	Dataset	Advantages and limitations
Su et al. [45]	Optimal shrinkage	79.25 ± 31.75 93.21 ± 14.31	P and T wave detection	Normalized mean amplitude error (-) 4.85 ± 8.33 0.22 ± 0.34	(semi)-Real, Synthetic on recordings	+ effective on pathological recordings - less effective with a significant amplitude of mECG
Behar et. al. [46]	ICA, πCA, JADE and SOBI ICA	—	P wave detection	—	Real	+ effective for arrhythmia determination - algorithm was very sensitive to noise
Andreotti et. al. [44]	BSS methods, TS, adaptive methods	86.4–99.9 77.4–96.0 87.1–97.9	QT, T/QRS QT, T/QRS QT, T/QRS	Coefficient of determination (-) 0.189, 0.098 0.846, 0.916 0.574, 0.812	Synthetic	+ tested at different noise levels - less effective on recordings with ectopic beats
Behar et al. [47]	Extended KF	—	QT	Median absolute error (ms) 4.00	Synthetic	+ single channel method - not tested on recordings with abnormalities
Clifford et al. [48]	KF framework	—	ST analysis	The root mean square error (%) 3.20	Real	+ without distorting clinical parameters - diminished patient activity by epidural, leading to easier extraction of fECG
Ionescu et al. [72]	FastICA, WT, FFT	—	QT, T/QRS	—	Synthetic	+ effective for recordings with low amplitude of fECG component - tested on only two recordings
Karvounis et al. [1]	Efficient variant of FastICA	94.79	T/QRS ratio, ST waveform classification	ACC (%) 92.49 79.87	Synthetic	+ effective ST waveform classification - not tested on recordings with abnormalities
Podziemski et al. [50]	TS	—	QT	—	Challenge 2013 dataset (mix)	+ effective even for very noisy recordings - not tested on recordings with abnormalities
Widatalla et al. [20]	Model based	—	QT	Difference (%) < 5.00	Real	+ tested on recordings with abnormalities - less effective for recordings with higher noise levels
Proposed algorithm	ICA-RLS	91.42–99.69	ST analysis	ACC (%) 1.52–89.60	Real	+ without distorting clinical parameters - not tested on recordings with abnormalities

- The authors in [48] tested the KF framework to extract the signal for the ST analysis. The authors used their own real records acquired from 32 women (gestational age: 35–41 weeks) for testing. The accuracy was determined using the root mean square error, which reached a value of 3.20%. The authors note a limitation of the study which is the use of epidural in almost all women during the signal acquisition, which could lead to a suppression of patient activity and made it easier to extract the fECG signal. In this study, real records were used for testing, however, these are different records than we used and an objective comparison is not possible.
- The combination of three methods (FastICA, WT, FFT) was tested in [72] to determine the length of the QT interval and the T/QRS ratio. The authors did not present any statistical evaluation, but according to them, this method is also suitable for the analysis of records with low amplitude of the fECG component. However, the method was tested only on two synthetic records.

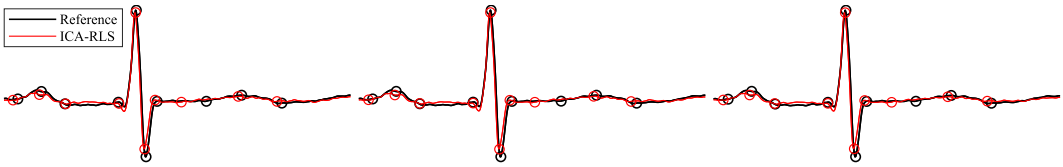

FIGURE 15. Detection and analysis of the estimated fECG signal features in comparison with reference signal obtained with fetal scalp electrode (the recording r08).

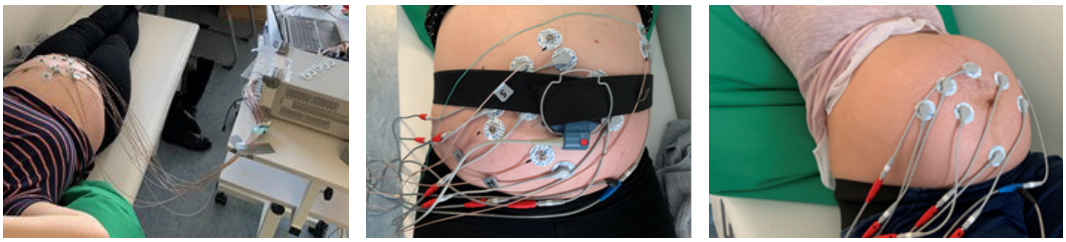

FIGURE 16. Example of the ongoing series of measurements of the research team from VSB–Technical University of Ostrava.

- The efficient variant of FastICA was tested in [1]. The authors presented the statistical evaluation for the determination of fHR, they achieved an average accuracy of 94.79%, which is a slightly worse result than that achieved by our proposed method. When evaluating the T/QRS ratio, an average accuracy of 92.49% was achieved, which is a significantly better result than we achieved. It should be noted that the efficient variant of FastICA was tested only on synthetic records and our proposed ICA-RLS on real records. In addition, the authors dealt with the ST waveform classification, which achieved an average accuracy of 79.87%.
- The authors in the [50] tested the template subtraction method and dealt with the length of the QT interval in the morphological analysis. No statistical evaluation was presented in the study, but according to the authors the method was efficient especially for partly noisy signals, but good results were also achieved for very noisy data.
- The model-based estimation was used in [20], where the authors primarily dealt with the analysis of the length of the QT interval. The authors used their own real records recorded on 58 women (gestational age: 20–41 weeks) for testing. The method was tested on normal (physiological) records, but also on records with abnormalities (e.g. bradycardia, tachycardia, heart anomalies, heart failure, placental dysfunction). A difference of $< 5.00\%$ was achieved between the reference and estimated values.

One of the challenges that future research should focus on is the analysis of other morphological elements that can help to further refine the fetal distress determination. Fig. 15 shows an example of detection and analysis of the extracted signal of a high quality. These signals could be used to perform morphological analysis of any part of the fECG cycle, especially the QT interval, which is significantly shortened due to fetal distress.

In order to verify the functionality of the proposed hybrid system in a larger number of patients, it will be necessary to create a quality database of real recordings. Ideally, the database should contain a sufficient number of recordings of adequate length covering possible variations in the fetal position and the pregnancy stage. Further research should be also focused on the effects of the electrode placement and system configuration. This would help in developing a new diagnostic system based on the simultaneous monitoring of fHR and NI-ST-analysis with the benefit of maintaining the non-invasiveness of the examination while refining the fetal distress diagnostics.

In our future research, our team intends to continue this work and focus primarily on creating our own aECG dataset with a large number of records for the purpose of testing and validating various approaches to fECG signal processing and extraction. Our dataset will contain records with various gestational age and different fetal positions. In addition to physiological records, pathological records will also be present. Thanks to this, various situations and effects can be tested and thus investigate which signal processing method is suitable for given purpose in clinical practice. Moreover, all records will contain information about the type of the signal (physiological or pathological), gestational age, fetal position and so on. Abdominal signals will be multichannel, at the same time, continuous measurement of direct fECG will be performed using a transvaginal fetal scalp electrode with simultaneous scanning using CTG. This will provide valid references for validating whether the extraction of fECG signals was successful in terms of both fHR monitoring and morphological analysis. In addition, reference annotations from the direct fECG signal will be created for each record. The annotations will contain the exact positions of fetal R peaks for possible testing of the accuracy of the fHR determination, which will also be possible to compare with the fHR trace provided by CTG device. Furthermore, the annotations

will contain reference markers for the ST analysis and thus the morphological analysis of the extracted fECG curve can be tested and evaluated. Fig. 16 shows a series of measurements already performed on several pregnant volunteers. The figure shows the use of CTG for continuous monitoring of fHR.

VI. CONCLUSION

This study investigated the effectiveness of the hybrid ICA-RLS method for the morphological analysis of the NI-fECG signal. Tests on real recordings from the ADFECGDB database have shown that in addition to accurate fHR estimation, it is also possible to perform non-invasive morphological analysis of the fECG signals. The primary objective of the study was to perform the ST segment analysis in order to increase the accuracy of fetal distress diagnosis. The ability to accurately determine fHR and perform ST segment analysis was assessed using objective quality indices such as ACC, SE, PPV, and F1, but also with a help of graphical evaluation methods (Bland-Altman plots and fHR traces). High accuracy of fHR estimation, reflected in the values of the mean μ within the range from 0.01 to 1.39 bpm and the mean $\pm 1.96\sigma$ from 1.76 to 14.08 bpm, was achieved for all eight patients examined. Based on the comparison with the results achieved using invasive means of fetal monitoring, the proposed algorithm has proven also its ability to perform the high quality ST segment analysis. For 7 out of 8 patients we were able to determine T/QRS ratio precisely with the values of the mean $|\mu|$ ranging from 0.0025 to 0.0307 and $\pm 1.96\sigma$ from 0.0043 to 0.1942. The results of this study demonstrate that morphological analysis can be performed on NI-fECG signal while achieving similar results as when direct fECG signal is used. The future research will aim to extend this study to the analysis of other fECG signal features, such as QT interval.

ETHICS STATEMENT

The study protocol was approved by the Ethical Committee of the Silesian Medical University, Katowice, Poland (NN-013-345/02). Subjects read the approved consent form and gave written informed consent to participate in the study.

REFERENCES

[1] E. C. Karvounis, M. G. Tsipouras, C. Papaloukas, D. G. Tsalikakis, K. K. Naka, and D. I. Fotiadis, "A non-invasive methodology for fetal monitoring during pregnancy," *Methods Inf. Med.*, vol. 49, no. 03, pp. 238–253, 2010.

[2] J. Jezewski, A. Pawlak, K. Horoba, J. Wrobel, R. Czabanski, and M. Jezewski, "Selected design issues of the medical cyber-physical system for telemonitoring pregnancy at home," *Microprocessors Microsyst.*, vol. 46, pp. 35–43, Oct. 2016.

[3] T. Y. Euliano, M. T. Nguyen, S. Darmanjian, S. P. McGorray, N. Euliano, A. Onkala, and A. R. Gregg, "Monitoring uterine activity during labor: A comparison of 3 methods," *Amer. J. Obstetrics Gynecol.*, vol. 208, no. 1, pp. 66.e1–66.e6, Jan. 2013.

[4] H. Y. Chen, S. P. Chauhan, C. V. Ananth, A. M. Vintzileos, and A. Z. Abuhamad, "Electronic fetal heart rate monitoring and its relationship to neonatal and infant mortality in the United States," *Amer. J. Obstetrics Gynecol.*, vol. 204, no. 6, pp. 491.e1–491.e10, 2011.

[5] T. P. Sartwelle, "Electronic fetal monitoring: A bridge too far," *J. Legal Med.*, vol. 33, no. 3, pp. 313–379, Jul. 2012.

[6] J. Wrobel, D. Roj, J. Jezewski, K. Horoba, T. Kupka, and M. Jezewski, "Evaluation of the robustness of fetal heart rate variability measures to low signal quality," *J. Med. Imag. Health Informat.*, vol. 5, no. 6, pp. 1311–1318, Nov. 2015.

[7] J. Jezewski, K. Horoba, D. Roj, J. Wrobel, T. Kupka, and A. Matonia, "Evaluating the fetal heart rate baseline estimation algorithms by their influence on detection of clinically important patterns," *Biocybernetics Biomed. Eng.*, vol. 36, no. 4, pp. 562–573, 2016.

[8] R. Czabanski, M. Jezewski, J. Wrobel, K. Horoba, and J. Jezewski, "A neuro-fuzzy approach to the classification of fetal cardiotocograms," in *Proc. 14th Nordic-Baltic Conf. Biomed. Eng. Med. Phys.*, vol. 20, R. Magjarevic, J. H. Nagel, A. Katashev, Y. Dekhtyar, and J. Spigulis, Eds. Berlin, Germany: Springer, 2008, pp. 446–449.

[9] J. Reinhard, B. R. Hayes-Gill, Q. Yi, H. Hatzmann, and S. Schiermeier, "Comparison of non-invasive fetal electrocardiogram to Doppler cardiotocogram during the 1st stage of labor," *J. Perinatal Med.*, vol. 38, no. 2, Jan. 2010.

[10] W. R. Cohen, S. Ommani, S. Hassan, F. G. Mirza, M. Solomon, R. Brown, B. S. Schifrin, J. M. Himsworth, and B. R. Hayes-Gill, "Accuracy and reliability of fetal heart rate monitoring using maternal abdominal surface electrodes: Maternal surface electrode fetal monitoring," *Acta Obstetricia et Gynecologica Scandinavica*, vol. 91, no. 11, pp. 1306–1313, Nov. 2012.

[11] J. Jezewski, J. Wrobel, A. Matonia, K. Horoba, R. Martinek, T. Kupka, and M. Jezewski, "Is abdominal fetal electrocardiography an alternative to Doppler ultrasound for FHR variability evaluation?" *Frontiers Physiol.*, vol. 8, p. 305, May 2017.

[12] I. Amer-Wahlin, S. Arulkumaran, H. Hagberg, K. Maršál, and G. Visser, "Fetal electrocardiogram: ST waveform analysis in intrapartum surveillance," *BJOG, Int. J. Obstetrics Gynaecology*, vol. 114, no. 10, pp. 1191–1193, Sep. 2007.

[13] I. Amer-Wåhlin, C. Hellsten, H. Norén, H. Hagberg, A. Herbst, I. Kjellmer, H. Lilja, C. Lindoff, M. Månsson, L. Mårtensson, P. Olofsson, A.-K. Sundström, and K. Maršál, "Cardiotocography only versus cardiotocography plus ST analysis of fetal electrocardiogram for intrapartum fetal monitoring: A swedish randomised controlled trial," *Lancet*, vol. 358, no. 9281, pp. 534–538, Aug. 2001.

[14] J. Westgate, M. Harris, J. S. H. Curnow, and K. R. Greene, "Plymouth randomized trial of cardiotocogram only versus ST waveform plus cardiotocogram for intrapartum monitoring in 2400 cases," *Amer. J. Obstetrics Gynecology*, vol. 169, no. 5, pp. 1151–1160, Nov. 1993.

[15] J. P. Neilson, "Fetal electrocardiogram (ECG) for fetal monitoring during labour," *Cochrane Database Systematic Rev.*, vol. 25, no. 1, Dec. 2015.

[16] Sameni, "A review of fetal ECG signal processing issues and promising directions," *Open Pacing, Electrophysiology Therapy J.*, Jan. 2010.

[17] G. D. Clifford, I. Silva, J. Behar, and G. B. Moody, "Non-invasive fetal ECG analysis," *Physiological Meas.*, vol. 35, no. 8, pp. 1521–1536, Aug. 2014.

[18] J. Jezewski, K. Horoba, A. Matonia, A. Gacek, and M. Bernys, "A new approach to cardiotocographic fetal monitoring based on analysis of bioelectrical signals," in *Proc. 25th Annu. Int. Conf. IEEE Eng. Med. Biol. Soc.*, Sep. 2003, pp. 3145–3148.

[19] M. A. Oudijk, A. Kwee, G. H. A. Visser, S. Blad, E. J. Meijboom, and K. G. Rosen, "The effects of intrapartum hypoxia on the fetal QT interval," *BJOG, Int. J. Obstetrics Gynaecology*, vol. 111, no. 7, pp. 656–660, Jul. 2004.

[20] N. Widatalla, Y. Kasahara, Y. Kimura, and A. Khandoker, "Model based estimation of QT intervals in non-invasive fetal ECG signals," *PLoS ONE*, vol. 15, no. 5, May 2020, Art. no. e0232769.

[21] B. F. Cuneo, J. F. Strasburger, and R. T. Wakai, "The natural history of fetal long QT syndrome," *J. Electrocardiology*, vol. 49, no. 6, pp. 807–813, Nov. 2016.

[22] J. Behar, T. Zhu, J. Oster, A. Niksch, D. Y. Mah, T. Chun, J. Greenberg, C. Tanner, J. Harrop, R. Sameni, J. Ward, A. J. Wolfberg, and G. D. Clifford, "Evaluation of the fetal QT interval using non-invasive fetal ECG technology," *Physiological Meas.*, vol. 37, no. 9, pp. 1392–1403, Sep. 2016.

[23] R. Martinek, R. Kahankova, J. Jezewski, R. Jaros, J. Mohylova, M. Fajkus, J. Nedoma, P. Janku, and H. Nazeran, "Comparative effectiveness of ICA and PCA in extraction of fetal ECG from abdominal signals: Toward non-invasive fetal monitoring," *Frontiers Physiol.*, vol. 9, p. 648, May 2018.

[24] R. Petrolis, V. Gintautas, and A. Krisciukaitis, "Multistage principal component analysis based method for abdominal ECG decomposition," *Physiological Meas.*, vol. 36, no. 2, pp. 329–340, Feb. 2015.
[25] Q. Yu, H. Yan, L. Song, W. Guo, H. Liu, J. Si, and Y. Zhao, "Automatic identifying of maternal ECG source when applying ICA in fetal ECG extraction," *Biocybernetics Biomed. Eng.*, vol. 38, no. 3, pp. 448–455, 2018.
[26] K. D. Desai and M. S. Sankhe, "A real-time fetal ECG feature extraction using multiscale discrete wavelet transform," in *Proc. 5th Int. Conf. Biomed. Eng. Informat.*, Chongqing, China, Oct. 2012, pp. 407–412.
[27] K. Assaleh, "Extraction of fetal electrocardiogram using adaptive neuro-fuzzy inference systems," *IEEE Trans. Biomed. Eng.*, vol. 54, no. 1, pp. 59–68, Jan. 2007.
[28] R. Martinek, R. Kahankova, H. Nazeran, J. Konecny, J. Jezewski, P. Janku, P. Bilik, J. Zidek, J. Nedoma, and M. Fajkus, "Non-invasive fetal monitoring: A maternal surface ECG electrode placement-based novel approach for optimization of adaptive filter control parameters using the LMS and RLS algorithms," *Sensors*, vol. 17, no. 5, p. 1154, May 2017.
[29] R. Jaros, R. Martinek, R. Kahankova, and J. Koziorek, "Novel hybrid extraction systems for fetal heart rate variability monitoring based on non-invasive fetal electrocardiogram," *IEEE Access*, vol. 7, pp. 131758–131784, 2019.
[30] K. Barnova, R. Martinek, R. Jaros, and R. Kahankova, "Hybrid methods based on empirical mode decomposition for non-invasive fetal heart rate monitoring," *IEEE Access*, vol. 8, pp. 51200–51218, 2020.
[31] M. Lukoševičius and V. Marozas, "Noninvasive fetal QRS detection using an echo state network and dynamic programming," *Physiological Meas.*, vol. 35, no. 8, pp. 1685–1697, Aug. 2014.
[32] L. Billeci and M. Varanini, "A combined independent source separation and quality index optimization method for fetal ECG extraction from abdominal maternal leads," *Sensors*, vol. 17, no. 5, p. 1135, May 2017.
[33] T. Kazmi, F. Radfer, and S. Khan, "ST analysis of the fetal ECG, as an adjunct to fetal heart rate monitoring in labour: A review," *Oman Med. J.*, vol. 26, no. 6, pp. 459–460, Nov. 2011.
[34] A. Sacco, J. Muglu, R. Navaratnarajah, and M. Hogg, "ST analysis for intrapartum fetal monitoring," *Obstetrician Gynaecologist*, vol. 17, no. 1, pp. 5–12, Jan. 2015.
[35] A. Daamouche, L. Hamami, N. Alajlan, and F. Melgani, "A wavelet optimization approach for ECG signal classification," *Biomed. Signal Process. Control*, vol. 7, no. 4, pp. 342–349, Jul. 2012.
[36] R. Kahankova, R. Martinek, R. Jaros, K. Behbehani, A. Matonia, M. Jezewski, and J. A. Behar, "A review of signal processing techniques for non-invasive fetal electrocardiography," *IEEE Rev. Biomed. Eng.*, vol. 13, pp. 51–73, 2020.
[37] M. J. Rooijakkers, S. Song, C. Rabotti, S. G. Oei, J. W. M. Bergmans, E. Cantatore, and M. Mischi, "Influence of electrode placement on signal quality for ambulatory pregnancy monitoring," *Comput. Math. Methods Med.*, vol. 2014, pp. 1–12, Feb. 2014.
[38] J. Behar, F. Andreotti, S. Zaunseder, Q. Li, J. Oster, and G. D. Clifford, "An ECG simulator for generating maternal-foetal activity mixtures on abdominal ECG recordings," *Physiological Meas.*, vol. 35, no. 8, pp. 1537–1550, Aug. 2014.
[39] J. Jezewski, A. Matonia, T. Kupka, D. Roj, and R. Czabanski, "Determination of fetal heart rate from abdominal signals: Evaluation of beat-to-beat accuracy in relation to the direct fetal electrocardiogram," *Biomedizinische Technik/Biomed. Eng.*, vol. 57, no. 5, pp. 383–394, Jan. 2012.
[40] A. L. Goldberger, L. A. N. Amaral, L. Glass, J. M. Hausdorff, P. C. Ivanov, R. G. Mark, J. E. Mietus, G. B. Moody, C.-K. Peng, and H. E. Stanley, "PhysioBank, PhysioToolkit, and PhysioNet: Components of a new research resource for complex physiologic signals," *Circulation*, vol. 101, no. 23, pp. e215–e220, Jun. 2000.
[41] L. Cordero and E. H. Hon, "Scalp abscess: A rare complication of fetal monitoring," *J. Pediatrics*, vol. 78, no. 3, pp. 533–537, Mar. 1971.
[42] D. M. Okada, A. W. Chow, and V. T. Bruce, "Neonatal scalp abscess and fetal monitoring: Factors associated with infection," *Amer. J. Obstetrics Gynecology*, vol. 129, no. 2, pp. 185–189, Sep. 1977.
[43] A. Salmelin, I. Wiklund, R. Bottinga, B. Brorsson, G. Ekman-Ordeberg, E. E. Grimfors, U. Hanson, M. Blom, and E. Persson, "Fetal monitoring with computerized ST analysis during labor: A systematic review and meta-analysis: Computerized ST analysis during labor," *Acta Obstetricia et Gynecologica Scandinavica*, vol. 92, no. 1, pp. 28–39, Jan. 2013.
[44] F. Andreotti, J. Behar, S. Zaunseder, J. Oster, and G. D. Clifford, "An open-source framework for stress-testing non-invasive foetal ECG extraction algorithms," *Physiological Meas.*, vol. 37, no. 5, pp. 627–648, May 2016.
[45] P.-C. Su, S. Miller, S. Idriss, P. Barker, and H.-T. Wu, "Recovery of the fetal electrocardiogram for morphological analysis from two trans-abdominal channels via optimal shrinkage," *Physiological Meas.*, vol. 40, no. 11, Dec. 2019, Art. no. 115005.
[46] J. A. Behar, L. Bonnemains, V. Shulgin, J. Oster, O. Ostras, and I. Lakhno, "Noninvasive fetal electrocardiography for the detection of fetal arrhythmias," *Prenatal Diagnosis*, vol. 39, no. 3, pp. 178–187, Feb. 2019.
[47] J. Behar, F. Andreotti, J. Oster, and G. D. Clifford, "A Bayesian filtering framework for accurate extracting of the non-invasive FECG morphology," in *Proc. Comput. Cardiol.*, Sep. 2014, pp. 53–56.
[48] G. Clifford, R. Sameni, J. Ward, J. Robinson, and A. J. Wolfberg, "Clinically accurate fetal ECG parameters acquired from maternal abdominal sensors," *Amer. J. Obstetrics Gynecol.*, vol. 205, no. 1, pp. 47.e1–47.e5, Jul. 2011.
[49] I. Silva, J. Behar, R. Sameni, T. Zhu, J. Oster, G. D. Clifford, and G. B. Moody, "Noninvasive fetal ECG: The physionet/computing in cardiology challenge 2013," in *Proc. Comput. Cardiol.*, Sep. 2013, pp. 149–152.
[50] P. Podziemski and J. Gieraltowski, "Fetal heart rate discovery: Algorithm for detection of fetal heart rate from noisy, noninvasive fetal ECG recordings," in *Proc. Comput. Cardiol.*, Sep. 2013, pp. 333–336.
[51] E. Castillo, D. P. Morales, G. Botella, A. García, L. Parrilla, and A. J. Palma, "Efficient wavelet-based ECG processing for single-lead FHR extraction," *Digit. Signal Process.*, vol. 23, no. 6, pp. 1897–1909, Dec. 2013.
[52] G. Liu and Y. Luan, "An adaptive integrated algorithm for non-invasive fetal ECG separation and noise reduction based on ICA-EEMD-WS," *Med. Biol. Eng. Comput.*, vol. 53, no. 11, pp. 1113–1127, Nov. 2015.
[53] R. Sameni, M. B. Shamsollahi, and C. Jutten, "Filtering electrocardiogram signals using the extended Kalman filter," in *Proc. IEEE Eng. Med. Biol. 27th Annu. Conf.*, Shanghai, China, Jan. 2005, pp. 5639–5642.
[54] D. Panigrahy and P. K. Sahu, "Extraction of fetal ECG signal by an improved method using extended Kalman smoother framework from single channel abdominal ECG signal," *Australas. Phys. Eng. Sci. Med.*, vol. 40, no. 1, pp. 191–207, Mar. 2017.
[55] R. Sameni, C. Jutten, and M. B. Shamsollahi, "What ICA provides for ECG processing: Application to noninvasive fetal ECG extraction," in *Proc. IEEE Int. Symp. Signal Process. Inf. Technol.*, Aug. 2006, pp. 656–661.
[56] R. Swarnalath and D. V. Prasad, "A novel technique for extraction of FECG using multi stage adaptive filtering," *J. Appl. Sci.*, vol. 10, no. 4, pp. 319–324, Feb. 2010.
[57] H. Hassanpour and A. Parsaei, "Fetal ECG extraction using wavelet transform," in *Proc. Int. Conf. Comput. Inteligence Modeling Control Autom. Int. Conf. Intell. Agents Web Technol. Int. Commerce (CIMCA)*, Sydney, NSW, Australia, Nov. 2006, p. 179.
[58] R. Martinek, R. Kahankova, J. Nedoma, M. Fajkus, and K. Cholevova, "Fetal ECG preprocessing using wavelet transform," in *Proc. 10th Int. Conf. Comput. Modeling Simulation (ICCMS)*, Sydney, NSW, Australia, 2018, pp. 39–43.
[59] S. Wu, Y. Shen, Z. Zhou, L. Lin, Y. Zeng, and X. Gao, "Research of fetal ECG extraction using wavelet analysis and adaptive filtering," *Comput. Biol. Med.*, vol. 43, no. 10, pp. 1622–1627, Oct. 2013.
[60] D. D. Taralunga, I. Gussi, and R. Strungaru, "A new method for fetal electrocardiogram denoising using blind source separation and empirical mode decomposition," *Revue Roumaine des Sci. Techn., serie Électrotechnique et Énergetique*, vol. 61, no. 1, pp. 94–98, 2016.
[61] P. Ghobadi Azbari, M. Abdolghaffar, S. Mohaqeqi, M. Pooyan, A. Ahmadian, and N. Ghanbarzadeh Gashti, "A novel approach to the extraction of fetal electrocardiogram based on empirical mode decomposition and correlation analysis," *Australas. Phys. Eng. Sci. Med.*, vol. 40, no. 3, pp. 565–574, Sep. 2017.

[62] A. Bin Queyam, S. Kumar Pahuja, and D. Singh, "Quantification of feto-maternal heart rate from abdominal ECG signal using empirical mode decomposition for heart rate variability analysis," *Technologies*, vol. 5, no. 4, p. 68, Oct. 2017.

[63] M. Niknazar, B. Rivet, and C. Jutten, "Fetal ECG extraction by extended state Kalman filtering based on single-channel recordings," *IEEE Trans. Biomed. Eng.*, vol. 60, no. 5, pp. 1345–1352, May 2013.

[64] M. Suganthy and S. Manjula, "Enhancement of SNR in fetal ECG signal extraction using combined SWT and WLSR in parallel EKF," *Cluster Comput.*, vol. 22, no. S2, pp. 3875–3881, Mar. 2019.

[65] E. Fotiadou and R. Vullings, "Multi-channel fetal ECG denoising with deep convolutional neural networks," *Frontiers Pediatrics*, vol. 8, p. 508, Aug. 2020.

[66] G. Camps-Valls, M. Martínez-Sober, E. Soria-Olivas, R. Magdalena-Benedito, J. Calpe-Maravilla, and J. Guerrero-Martínez, "Foetal ECG recovery using dynamic neural networks," *Artif. Intell. Med.*, vol. 31, no. 3, pp. 197–209, Jul. 2004.

[67] M. Nasiri, K. Faez, and A. M. Nasrabadi, "A new method for extraction of fetal electrocardiogram signal based on adaptive nero-fuzzy inference system," in *Proc. IEEE Int. Conf. Signal Image Process. Appl. (ICSIPA)*, Kuala Lumpur, Malaysia, Nov. 2011, pp. 456–461.

[68] J. Behar, A. E. Johnson, J. Oster, and G. Clifford, "An echo state neural network for foetal ECG extraction optimised by random search," in *Proc. Adv. Neural Inf. Process. Syst*, 2013, pp. 1–5.

[69] V. Zarzoso and A. K. Nandi, "Noninvasive fetal electrocardiogram extraction: Blind separation versus adaptive noise cancellation," *IEEE Trans. Biomed. Eng.*, vol. 48, no. 1, pp. 12–18, 2001.

[70] A. Gupta, M. C. Srivastava, V. Khandelwal, and A. Gupta, "A novel approach to fetal ECG extraction and enhancement using blind source separation (BSS-ICA) and adaptive fetal ECG enhancer (AFE)," in *Proc. 6th Int. Conf. Inf., Commun. Signal Process.*, Singapore, 2007, pp. 1–4.

[71] M. Kotas, "Combined application of independent component analysis and projective filtering to fetal ECG extraction," *Biocybern. Biomed. Eng.*, vol. 28, no. 1, p. 75, 2008.

[72] V. Ionescu, "Fetal ECG extraction from multichannel abdominal ECG recordings for health monitoring during labor," *Procedia Technol.*, vol. 22, pp. 682–689, 2016.

[73] R. Martín-Clemente, J. L. Camargo-Olivares, S. Hornillo-Mellado, M. Elena, and I. Román, "Fast technique for noninvasive fetal ECG extraction," *IEEE Trans. Biomed. Eng.*, vol. 58, no. 2, pp. 227–230, Feb. 2011.

[74] P. P. Kanjilal, S. Palit, and G. Saha, "Fetal ECG extraction from single-channel maternal ECG using singular value decomposition," *IEEE Trans. Biomed. Eng.*, vol. 44, no. 1, pp. 51–59, 1997.

[75] M. Varanini, G. Tartarisco, L. Billeci, A. Macerata, G. Pioggia, and R. Balocchi, "A multi-step approach for non-invasive fetal ECG analysis," in *Proc. Comput. Cardiol.*, Sep. 2013, pp. 281–284.

[76] M. Kotas, J. Giraldo, S. H. Contreras-Ortiz, and G. I. B. Lasprilla, "Fetal ECG extraction using independent component analysis by jade approach," in *Proc. 13th Int. Conf. Med. Inf. Process. Anal.*, J. Brieva, J. D. García, N. Lepore, and E. Romero, Eds. San Andres Island, Colombia: SPIE, Nov. 2017, p. 55.

[77] K. Surya, K. K. Abdul Majeed, and R. V. Ravi, "Diagnosis of fetal arrhythmia using JADE algorithm," in *Proc. 7th Int. Conf. Smart Struct. Syst. (ICSSS)*, Chennai, India, Jul. 2020, pp. 1–5.

[78] L. Yuan, Z. Zhou, Y. Yuan, and S. Wu, "An improved FastICA method for fetal ECG extraction," *Comput. Math. Methods Med.*, vol. 2018, pp. 1–7, May 2018.

[79] Y. Wang, Y. Fu, and Z. He, "Fetal electrocardiogram extraction based on fast ICA and wavelet denoising," in *Proc. 2nd IEEE Adv. Inf. Manage., Communicates, Electron. Autom. Control Conf. (IMCEC)*, Xi'an, China, May 2018, pp. 466–469.

[80] J. J. R. Immanuel, V. Prabhu, V. J. Christopheraj, D. Sugumar, and P. T. Vanathi, "Separation of maternal and fetal ECG signals from the mixed source signal using FASTICA," *Procedia Eng.*, vol. 30, pp. 356–363, Jan. 2012.

[81] J. L. Camargo-Olivares, R. Martín-Clemente, S. Hornillo-Mellado, M. M. Elena, and I. Román, "The maternal abdominal ECG as input to MICA in the fetal ECG extraction problem," *IEEE Signal Process. Lett.*, vol. 18, no. 3, pp. 161–164, Mar. 2011.

[82] D. Taralunga, M. Ungureanu, R. Strungaru, and W. Wolf, "Performance comparison of four ICA algorithms applied for fECG extraction from transabdominal recordings," in *Proc. Int. Symp. Signals, Circuits Syst. (ISSCS)*, Iasi, Romania, Jun. 2011, pp. 1–4.

[83] D. A. Ramli, Y. H. Shiong, and N. Hassan, "Blind source separation (BSS) of mixed maternal and fetal electrocardiogram (ECG) signal: A comparative study," *Procedia Comput. Sci.*, vol. 176, pp. 582–591, Jan. 2020.

[84] P. J. He, X. M. Chen, Y. Liang, and H. Z. Zeng, "Extraction for fetal ECG using single channel blind source separation algorithm based on multi-algorithm fusion," in *Proc. MATEC Web Conf.*, vol. 44, p. 01026, 2016.

[85] S. Ziani and Y. El Hassouani, "Fetal electrocardiogram analysis based on LMS adaptive filtering and complex continuous wavelet 1-D," in *Big Data and Networks Technologies*, vol. 81, Y. Farhaoui, Ed. Cham, Switzerland: Springer, 2020, pp. 360–366.

[86] R. Martinek, R. Kahankova, H. Skutova, P. Koudelka, J. Zidek, and J. Koziorek, "Adaptive signal processing techniques for extracting abdominal fetal electrocardiogram," in *Proc. 10th Int. Symp. Commun. Syst., Netw. Digit. Signal Process. (CSNDSP)*, Prague, Czech Republic, Jul. 2016, pp. 1–6.

[87] J. Behar, A. Johnson, G. D. Clifford, and J. Oster, "A comparison of single channel fetal ECG extraction methods," *Ann. Biomed. Eng.*, vol. 42, no. 6, pp. 1340–1353, Jun. 2014.

[88] S.-J. Liu, D.-L. Liu, J.-Q. Zhang, and Y.-J. Zeng, "Extraction of fetal electrocardiogram using recursive least squares and normalized least mean squares algorithms," in *Proc. 3rd Int. Conf. Adv. Comput. Control*, Harbin, China, Jan. 2011, pp. 333–336.

[89] D. Ayres-de-Campos, C. Y. Spong, E. Chandraharan, "FIGO consensus guidelines on intrapartum fetal monitoring: Cardiotocography," *Int. J. Gynecology Obstetrics*, vol. 131, no. 1, pp. 13–24, Oct. 2015.

[90] F. News, "Guidelines for the use of fetal monitoring," *Int. J. Gynaecol Obstet*, vol. 25, no. 1, pp. 67–159, 1987.

[91] P. Olofsson, H. Norén, and A. Carlsson, "New FIGO and swedish intrapartum cardiotocography classification systems incorporated in the fetal ECG ST analysis (STAN) interpretation algorithm: Agreements and discrepancies in cardiotocography classification and evaluation of significant ST events," *Acta Obstetricia et Gynecologica Scandinavica*, vol. 97, no. 2, pp. 219–228, Feb. 2018.

[92] D. M. F. Gibb and S. Arulkumaran, *Fetal Monitoring in Practice*, 4th ed. London, U.K.: Churchill Livingstone, 2017.

[93] I. Amer-Wahlin, A. Ugwumadu, B. M. Yli, A. Kwee, S. Timonen, V. Cole, D. Ayres-de-Campos, G.-E. Roth, C. Schwarz, L. A. Ramenghi, T. Todros, V. Ehlinger, and C. Vayssiere, "Fetal electrocardiography ST-segment analysis for intrapartum monitoring: A critical appraisal of conflicting evidence and a way forward," *Amer. J. Obstetrics Gynecol.*, vol. 221, no. 6, pp. e11.577–e11.601, Dec. 2019.

[94] H. Lilja, K. R. Greene, K. Karlsson, and K. G. Rosen, "ST waveform changes of the fetal electrocardiogram during labour—A clinical study," *BJOG, Int. J. Obstetrics Gynaecol.*, vol. 92, no. 6, pp. 611–617, Jun. 1985.

[95] S. Arulkumaran, H. Lilja, K. Lindecrantz, S. S. Ratnam, A. S. Thavarasah, and K. G. Rosén, "Fetal ECG waveform analysis should improve fetal surveillance in labour," *J. Perinatal Med.*, vol. 18, no. 1, pp. 13–22, Jan. 1990.

[96] K. G. Rosen, "Alterations in the fetal electrocardiogram as a sign of fetal asphyxia–experimental data with a clinical implementation," *J. Perinatal Med.*, vol. 14, no. 6, pp. 355–363, 1986.

[97] P. Christian and B. Davidsen, "The significance of the foetal electrocardiogram during labour with detailed report of one case," *Acta Obstetricia et Gynecologica Scandinavica*, vol. 50, no. 1, pp. 45–49, Jan. 1971.

[98] G. Pardi, E. Tucci, A. Uderzo, and D. Zanini, "Fetal electrocardiogram changes in relation to fetal heart rate patterns during labor," *Amer. J. Obstetrics Gynecology*, vol. 118, no. 2, pp. 243–250, Jan. 1974.

[99] L.-Y. Chen and C.-J. Lu, "An improved independent component analysis algorithm based on artificial immune system," *Int. J. Mach. Learn. Comput.*, vol. 3, no. 1, pp. 93–97, 2013.

[100] E. Sulas, M. Urru, R. Tumbarello, L. Raffo, and D. Pani, "Systematic analysis of single- and multi-reference adaptive filters for non-invasive fetal electrocardiography," *Math. Biosci. Eng.*, vol. 17, no. 1, pp. 286–308, 2020.

[101] A. Hyvärinen and E. Oja, "Independent component analysis: Algorithms and applications," *Neural Netw.*, vol. 13, nos. 4–5, pp. 411–430, Jun. 2000.

[102] J. Benesty and T. Gänsler, "New insights into the RLS algorithm," *EURASIP J. Adv. Signal Process.*, vol. 2004, no. 3, Dec. 2004, Art. no. 243857.
[103] A. Matonia, J. Jezewski, T. Kupka, M. Jezewski, K. Horoba, J. Wrobel, R. Czabanski, and R. Kahankowa, "Fetal electrocardiograms, direct and abdominal with reference heartbeat annotations," *Sci. Data*, vol. 7, no. 1, p. 200, Dec. 2020.
[104] R. Kahankova, "Advanced signal processing methods for non-invasive fetal electrocardiogram extraction," Ph.D. dissertation, VSB Tech. Univ. Ostrava, Ostrava, Czech Republic, 2019.
[105] R. Jaros, R. Martinek, R. Kahankova, and K. Barnova. (Jan. 2021). *ST Annotations of ADFECGDB Database*. [Online]. Available: https://ieee-dataport.org/documents/st-annotations-adfecgdb-database
[106] C. Li, C. Zheng, and C. Tai, "Detection of ECG characteristic points using wavelet transforms," *IEEE Trans. Biomed. Eng.*, vol. 42, no. 1, pp. 21–28, 1995.
[107] A. Ghaffari, H. Golbayani, and M. Ghasemi, "A new mathematical based QRS detector using continuous wavelet transform," *Comput. Electr. Eng.*, vol. 34, no. 2, pp. 81–91, Mar. 2008.
[108] P. Du, W. A. Kibbe, and S. M. Lin, "Improved peak detection in mass spectrum by incorporating continuous wavelet transform-based pattern matching," *Bioinformatics*, vol. 22, no. 17, pp. 2059–2065, Sep. 2006.
[109] E. Chandraharan, Ed., *Handbook CTG Interpretation: From Patterns to Physiology*. Cambridge, U.K.: Cambridge Univ. Press, 2017.
[110] M. Elgendi, B. Eskofier, and D. Abbott, "Fast t wave detection calibrated by clinical knowledge with annotation of p and t waves," *Sensors*, vol. 15, no. 7, pp. 17693–17714, Jul. 2015.
[111] J. Pan and W. J. Tompkins, "A real-time QRS detection algorithm," *IEEE Trans. Biomed. Eng.*, vols. BME–32, no. 3, pp. 230–236, Mar. 1985.
[112] S. Verma and R. Vashistha, "Efficient RR-interval time series formulation for heart rate detection," in *Multimedia, Signal Processing and Communication Technologies (IMPACT), 2013 International Conference on*, Aligarh, India, Nov. 2013, pp. 84–87.
[113] G. B. Moody and R. G. Mark, "The impact of the MIT-BIH arrhythmia database," *IEEE Eng. Med. Biol. Mag.*, vol. 20, no. 3, pp. 45–50, May/Jun. 2001.
[114] J. Arteaga-Falconi, H. Al Osman, and A. El Saddik, "R-peak detection algorithm based on differentiation," in *Proc. IEEE 9th Int. Symp. Intell. Signal Process. (WISP)*, Siena, Italy, May 2015, pp. 1–4.
[115] S. Ktata, K. Ouni, and N. Ellouze, "ECG signal maxima detection using wavelet transform," in *Proc. IEEE Int. Symp. Ind. Electron.*, Montreal, QC, Canada, Jul. 2006, pp. 700–703.
[116] R. Haddadi, E. Abdelmounim, M. El Hanine, and A. Belaguid, "Discrete wavelet transform based algorithm for recognition of QRS complexes," in *Proc. Int. Conf. Multimedia Comput. Syst. (ICMCS)*, Marrakech, Morocco, Apr. 2014, pp. 375–379.
[117] J. P. Martinez, R. Almeida, S. Olmos, A. P. Rocha, and P. Laguna, "A wavelet-based ECG delineator: Evaluation on standard databases," *IEEE Trans. Biomed. Eng.*, vol. 51, no. 4, pp. 570–581, Apr. 2004.
[118] K. F. Tan, "Detection of the QRS complex, p wave and t wave in electrocardiogram," in *Proc. 1st Int. Conf. Adv. Med. Signal Inf. Process.*, Bristol, U.K., 2000, pp. 41–47.
[119] P. Laguna, R. Mark, A. Goldberg, and G. Moody, "A database for evaluation of algorithms for measurement of QT and other waveform intervals in the ECG," in *Proc. Comput. Cardiol.*, Lund, Sweden, 1997, pp. 673–676.
[120] S. Lixin, W. Yuhong, and G. Lili, "A p-wave detection method in ECG based on multi-feature and wavelet-amplitude threshold," in *Proc. Int. Conf. Inf. Commun. Technol. (ICT)*. Nanjing, China: Institution of Engineering and Technology, 2014, p. 3.093–3.093.
[121] M. Rakshit, D. Panigrahy, and P. K. Sahu, "EKF with PSO technique for delineation of p and t wave in electrocardiogram(ECG) signal," in *Proc. 2nd Int. Conf. Signal Process. Integr. Netw. (SPIN)*, Noida, India, Feb. 2015, pp. 696–701.
[122] C. Bock, "ECG signal analysis based on the wavelet transform," Ph.D. dissertation, JKU Linz, Linz, Austria, 2015.
[123] M. Chrobak and J. Kozumplik, "Comparison of the most widely used algorithms for the detection of QT interval," *Elektrorevue*, vol. 15, no. 4, pp. 233–237, 2013.

RADEK MARTINEK (Member, IEEE) was born in Czech Republic, in 1984. He received the master's degree in information and communication technology from the VSB—Technical University of Ostrava, in 2009. In 2014, he successfully defended his dissertation thesis titled "The Use of Complex Adaptive Methods of Signal Processing for Refining the Diagnostic Quality of the Abdominal Fetal Electrocardiogram." Since 2012 he has been a Research Fellow with the VSB—Technical University of Ostrava. In 2017, he became an Associate Professor in technical cybernetics after defending the habilitation thesis titled "Design and Optimization of Adaptive Systems for Applications of Technical Cybernetics and Biomedical Engineering Based on Virtual Instrumentation." He has been an Associate Professor with the VSB—Technical University of Ostrava, since 2017. His current research interests include digital signal processing (linear and adaptive filtering, soft computing artificial intelligence and adaptive fuzzy systems, non-adaptive methods, biological signal processing, and digital processing of speech signals); wireless communications (software-defined radio); and power quality improvement. He has more than 200 journal and conference papers in his research areas.

RADANA KAHANKOVA was born in Opava, Czech Republic, in 1991. She received the bachelor's degree and the master's degree in biomedical engineering from the Department of Cybernetics and Biomedical Engineering, VSB—Technical University of Ostrava, in 2014 and 2016, respectively, and the Ph.D. degree in technical cybernetics, in 2019. Her current research interest includes improving the quality of electronic fetal monitoring.

RENE JAROS was born in Ostrava, Czech Republic, in 1992. He received the bachelor's degree and the master's degree in biomedical engineering from the Department of Cybernetics and Biomedical Engineering, VSB—Technical University of Ostrava, in 2015 and 2017, respectively, and the Ph.D. degree in technical cybernetics, in 2019. His research interest includes fetal electrocardiography (fECG) extraction by using hybrid methods.

KATERINA BARNOVA was born in Ostrava, Czech Republic, in 1993. She received the master's degree from the Department of Cybernetics and Biomedical Engineering, VSB—Technical University of Ostrava, in 2019, where she is currently pursuing the Ph.D. degree in technical cybernetics. Her research interest includes advanced signal processing methods, especially for fetal electrocardiography (fECG) extraction.

ADAM MATONIA was born in Poland, in 1975. He received the M.Sc. degree in electronic engineering and the Ph.D. degree in biocybernetics and biomedical engineering from the Silesian University of Technology, Gliwice, Poland, in 2000 and 2018, respectively. He is currently the Project Leader with the Biomedical Signal Processing Department, Łukasiewicz Research Network—Institute of Medical Technology and Equipment, Zabrze, Poland. His research interests include fetal electrocardiography, electrohysterography, mobile biomedical instrumentations, and software development for computerized fetal monitoring systems. He is a member of the Polish Society of Biomedical Engineering. He was a fellowship holder of the Foundation for Polish Science in 2005.

MICHAL JEZEWSKI was born in Zabrze, Poland, in 1982. He received the M.Sc. degree in computer science and the Ph.D. degree in electronics from the Silesian University of Technology, Gliwice, Poland, in 2006 and 2011, respectively. He is currently with the Department of Cybernetics, Nanotechnology and Data Processing, Silesian University of Technology, Gliwice, Poland. His research interests include biomedical signal processing and computational intelligence methods with emphasis on fuzzy clustering and fuzzy classifiers. He is a member of the Polish Society of Theoretical and Applied Electrotechnics.

ROBERT CZABANSKI was born in Tychy, Poland. He received the M.Sc. and Ph.D. degrees in electronics and the D.Sc. degree in biocybernetics and biomedical engineering from the Silesian University of Technology, Gliwice, Poland, in 1997, 2003, and 2018, respectively. He is currently with the Department of Cybernetics, Nanotechnology and Data Processing, Silesian University of Technology, Gliwice, Poland. His research interests include fuzzy and neuro-fuzzy modeling, learning theory, and biomedical signal processing. He is a member of the Polish Society of Theoretical and Applied Electrotechnics.

KRZYSZTOF HOROBA was born in Poland, in 1968. He received the M.S. degree in electronic engineering from the Silesian University of Technology, Gliwice, Poland, in 1993, the Ph.D. degree in medical science from the University of Medical Sciences, Poznan, Poland, in 2001, and the D.Sc. degree in biocybernetics and biomedical engineering from the Silesian University of Technology, in 2017. He is currently the Head of the Biomedical Signals Processing Department, Łukasiewicz Research Network—Institute of Medical Technology and Equipment, Zabrze, Poland. His research interests include fetal electrocardiography, electrohysterography, as well as the software development of the computerized fetal monitoring systems. He is a member of the Polish Society of Biomedical Engineering. He was a fellowship holder of the Foundation for Polish Science in 1997.

JANUSZ JEZEWSKI (Senior Member, IEEE) was born in Zabrze, Poland. He received the M.Sc. degree in electronics from the Silesian University of Technology, Gliwice, Poland, the Ph.D. degree in biological sciences from the University of Medical Sciences, Poznan, Poland, and the D.Sc. degree in biocybernetics and biomedical engineering from the Institute of Biocybernetics and Biomedical Engineering, Polish Academy of Sciences, Warsaw, Poland. He is currently the Director for Science of the Łukasiewicz Research Network—Institute of Medical Technology and Equipment, Zabrze. He has authored or coauthored more than 300 international journal and conference papers. His research interests include biomedical instrumentation, digital signal processing, and application of computational intelligence in medical cyber-physical systems. He is a member of the Committee of Biocybernetics and Biomedical Engineering of the Polish Academy of Sciences, the Polish Society of Biomedical Engineering, the Institute of Physics and Engineering in Medicine, and the European Society for Engineering and Medicine. He received the title of Professor conferred by the President of the Republic of Poland.